

# Leptonic CP Phase Determination from Fisher Information in $\text{NO}\nu\text{A}$ and T2K

Neetu Raj Singh Chundawat<sup>1,2,\*</sup> Luis A. Delgadillo<sup>1,2,†</sup> and Yu-Feng Li<sup>1,3,‡</sup>

<sup>1</sup>*Institute of High Energy Physics, Chinese Academy of Sciences, Beijing 100049, China*

<sup>2</sup>*Kaiping Neutrino Research Center, Guangdong 529386, China*

<sup>3</sup>*School of Physical Sciences, University of Chinese Academy of Sciences, Beijing 100049, China*

## Abstract

The precise determination of the leptonic CP phase ( $\delta_{\text{CP}}$ ) remains one of the central objectives of current and future long-baseline (LBL) neutrino oscillation experiments. Quantum estimation theory provides a natural framework to quantify the ultimate precision limits for estimating physical parameters encoded in quantum states. In this work, we employ the quantum Fisher information to investigate how much information about  $\delta_{\text{CP}}$  is intrinsically encoded in neutrino states and how efficiently it is extracted in present LBL experiments such as T2K and  $\text{NO}\nu\text{A}$ . We first analyze the intrinsic quantum sensitivity of neutrino and antineutrino states and demonstrate how matter effects generate a neutrino mass-ordering dependent information structure. To compare the intrinsic information content of the quantum state with the information experimentally accessible through flavor measurements, we compute the event-level Fisher information from reconstructed event spectra using Poisson statistics. We find that both experiments extract only a small fraction of the total information available in the underlying quantum state. This extraction efficiency becomes particularly suppressed near maximally CP-violating regions, where the reconstructed event spectra exhibit reduced sensitivity to small variations in  $\delta_{\text{CP}}$ . Our analysis provides a complementary information-theoretic perspective on precise estimation of oscillation parameters in LBL neutrino experiments.

---

\* [chundawat@ihep.ac.cn](mailto:chundawat@ihep.ac.cn)

† [ldelgadillof@ihep.ac.cn](mailto:ldelgadillof@ihep.ac.cn)

‡ [liyufeng@ihep.ac.cn](mailto:liyufeng@ihep.ac.cn)

## I. INTRODUCTION

The discovery of neutrino oscillations has provided the first definitive evidence for physics beyond the Standard Model (SM) [1, 2]. The Pontecorvo-Maki-Nakagawa-Sakata (PMNS) mixing matrix, which relates flavor and mass eigenstates, is parameterized by three mixing angles ( $\theta_{12}, \theta_{13}, \theta_{23}$ ) and a single Dirac CP-violating phase  $\delta_{\text{CP}}$  [3, 4]. Hence, the observation of a non-zero  $\delta_{\text{CP}}$  would constitute a violation of CP symmetry in the lepton sector, a potential ingredient in explaining the matter-antimatter asymmetry of the universe.

Over last decades, accelerator-based neutrino experiments have played a central role in the development of particle physics [5, 6]. The current generation of long-baseline (LBL) experiments, Tokai-to-Kamioka (T2K) in Japan ( $L = 295$  km) [7] and the NuMI Off-Axis  $\nu_e$  Appearance ( $\text{NO}\nu\text{A}$ ) in the USA ( $L = 810$  km) [8], are at the forefront of research in neutrino physics. While both experiments employ high-intensity  $\nu_\mu$  beams and measure  $\nu_e$  appearance, their distinct baselines and detector technologies yield complementary sensitivities. For instance, T2K uses a lower-energy beam ( $\sim 0.6$  GeV) and is sensitive to the first oscillation maximum, whereas  $\text{NO}\nu\text{A}$  provides a higher-energy beam ( $\sim 2$  GeV) where matter effects are significant.

Recently, a slight tension has emerged in the combined interpretation of their data. The T2K collaboration reports a preference for  $\delta_{\text{CP}} \sim 1.5\pi$  [9] under normal neutrino mass ordering, while  $\text{NO}\nu\text{A}$  data favor  $\delta_{\text{CP}} \sim 0.9\pi$  [10]. The latest joint analysis from the two experiments, while resolving some degeneracies, still yields constrained but potentially conflicting intervals [11]. Some explanations for this discrepancy range from statistical fluctuations to systematic uncertainties in neutrino flux or cross-section models, or even hints of physics beyond the Standard Model (BSM) such as neutrino non-standard interactions [12, 13]. Thus, the current situation in the neutrino sector therefore motivates a more fundamental question: how much information about the oscillation parameters can be extracted from a given experiment?

Information has appeared as an increasingly important concept in physics, particularly following the pioneering work of Jaynes [14]. The Cramér-Rao bound [15] states that the achievable precision in estimating a physical parameter is determined by the information encoded in the measurement outcomes and improves with increasing statistics. This information about the parameter can be quantitatively characterized by the Fisher information [16]. Recently, the extension of classical Fisher information to its quantum counterpart, known as Quantum Fisher Information (QFI), has emerged within the framework of quantum estimation theory [17–21]. The QFI naturally quantifies the sensitivity of a quantum state to changes in a parameter and determines the ultimate precision of its estimation via the Quantum Cramér-Rao bound (QCRB). In quantum metrology, it sets the fundamental limit on the achievable precision using quantum resources, enabling sensitivities beyond classical bounds. More recently, its scope has expanded to diverse areas of physics, including neutrino physics [22–27]. Apart from quantum estimation theory, several studies have explored the role of other quantum information theoretic quantities in neutrino oscillations [28–46].

In neutrino oscillations, the measurement process can be formulated within the most general framework of quantum measurements, namely positive operator-valued measures (POVMs) [47]. Within this description, neutrino detection is effectively represented as a set of flavor measurements corresponding to a restricted class of operators acting on the neutrino state. The Fisher information associated with this POVM quantifies the amount of information about the underlying oscillation parameters that is accessible through physically

realizable measurements. In particular, for standard neutrino oscillation experiments, this corresponds to the information that can be extracted from flavor measurements alone.

In neutrino detectors, the comparison between the neutrino state and the observables is not a simple projection onto flavor eigenstates, but also involves detector-specific effects such as energy binning, finite energy resolution, and backgrounds. The Fisher information corresponding to the measurements not only characterizes the sensitivity of the parameters under consideration but also highlights the limitations imposed by the detector itself, as compared to the case of perfect flavor measurements. In this work, we address the question of how much information is extracted in LBL experiments such as NO $\nu$ A and T2K by quantifying both the intrinsic and experimentally accessible information content associated with physical measurements, and studying how this information is related to the precision achieved in these experiments. Our approach provides a complementary perspective by analyzing the experimentally extractable information associated with neutrino oscillation parameters, particularly the leptonic CP-violating phase, and comparing it with the underlying QFI encoded in the propagated neutrino state for the same parameter.

The structure of the paper is organized as follows. In Sec. II, we introduce the Fisher Information formalism and discuss its relevant properties. In Sec. III, we describe the methodology adopted in the present work. Sec. IV is devoted to the experimental configurations and simulation setup for the T2K and NO $\nu$ A experiments. In Sec. V, we present the results and discussions. Finally, we summarize our main conclusions in Sec. VI.

## II. FISHER INFORMATION

### A. Quantum Fisher Information

A central result in estimation theory is the Cramér-Rao bound, which states that the uncertainty of any unbiased estimator  $\hat{\alpha}$  is bounded from below as

$$\Delta\hat{\alpha} \geq \frac{1}{\sqrt{N F(\alpha)}}, \quad (1)$$

where  $N$  denotes the number of independent measurements and

$$F(\alpha) = \sum_x \frac{1}{P(x|\alpha)} \left( \frac{\partial P(x|\alpha)}{\partial \alpha} \right)^2 \quad (2)$$

is the Fisher information. Here, the sum extends to all possible measurement outcomes  $x$ . The factor  $1/\sqrt{N}$  in Eq. (1) reflects the statistical improvement obtained from repeated independent measurements.

The Fisher information obtained from any measurement is bounded above by the QFI by maximizing over all the possible POVM in quantum mechanics, leading to the QCRB. The QFI depends only on the quantum state that describes the system and is independent of the specific measurement performed. It is therefore interpreted as the maximum amount of information about the parameter  $\alpha$  that can, in principle, be extracted from the quantum state, i.e.,

$$F_Q[\hat{\rho}(\alpha)] = \max_{\{\hat{E}_x\}} F(\alpha). \quad (3)$$

where  $\hat{E}_x$  are the projectors that correspond to different POVMs. For a pure state  $|\psi(\alpha)\rangle$ , the QFI takes the simplified form

$$F_Q^{\text{pure}}(\alpha) = 4 \left( \langle \partial_\alpha \psi | \partial_\alpha \psi \rangle - |\langle \psi | \partial_\alpha \psi \rangle|^2 \right), \quad (4)$$

where  $|\partial_\alpha \psi\rangle \equiv \frac{\partial}{\partial \alpha} |\psi\rangle$ .

## B. Convexity and Additivity

Both the QFI and the classical Fisher information satisfy several important mathematical properties. We list two of the most relevant properties that are used in our analysis below.

*Convexity:* For a statistical mixture of states  $\hat{\rho}_i(\alpha)$  with probabilities  $p_i$ , satisfying  $\sum_i p_i = 1$ , the QFI obeys

$$F_Q \left( \sum_i p_i \hat{\rho}_i(\alpha) \right) \leq \sum_i p_i F_Q(\hat{\rho}_i(\alpha)). \quad (5)$$

Similarly, the statistical mixture of states with weights  $p_i$ , the Fisher information satisfies

$$F(\alpha) \leq \sum_i p_i F_i(\alpha). \quad (6)$$

This reflects the fact that statistical mixing of quantum states does not enhance the attainable estimation precision.

*Additivity:* For  $N$  independent subsystems undergoing independent measurements or  $N$  uncorrelated events, the total Fisher information is given by the sum of the individual contributions,

$$F(\alpha) = \sum_{i=1}^N F_i(\alpha), \quad (7)$$

where  $F_i(\alpha)$  represents the Fisher information associated with the  $i$ -th subsystem.

For identically prepared and independent systems, this expression simplifies to

$$F(\alpha) = N F^{(1)}(\alpha), \quad (8)$$

where  $F^{(1)}(\alpha)$  denotes the Fisher information for a single subsystem. As a result, the Cramér-Rao bound scales similar to as given in Eq. (1).

A similar additivity property holds for the QFI. For  $N$  independent quantum states  $\hat{\rho}^{(i)}(\alpha)$ , one obtains

$$F_Q \left[ \bigotimes_{i=1}^N \hat{\rho}^{(i)}(\alpha) \right] = \sum_{i=1}^N F_Q[\hat{\rho}^{(i)}(\alpha)]. \quad (9)$$

In the special case of  $N$  identical copies  $\hat{\rho}(\alpha)$ , the total QFI reduces to

$$F_Q^{\text{tot}}(\alpha) = N F_Q[\hat{\rho}(\alpha)]. \quad (10)$$

### C. Flavor measurement as a POVM

The neutrinos in the experiments are detected by the final flavour of charged lepton produced via charged current interactions of neutrinos. This measurement process can be described in quantum mechanics by a specific POVM,  $\{\hat{E}_x\}$ , associated with flavor detection. For a system described by  $\hat{\rho}(\alpha)$ , the probability to obtain  $x$  can be written as,  $P(x|\alpha) = \text{Tr}[\hat{\rho}(\alpha)\hat{E}_x]$ . Thus, all measurement outcomes and their associated probabilities are determined by the pair  $\{\hat{\rho}(\alpha), \hat{E}_x\}$ .

In many physics scenarios, any quantum measurement can be approximated as an effective two-outcome POVM ( $\hat{E}_1, \hat{E}_2 = \mathbb{I} - \hat{E}_1$ ), for this case, the Fisher information corresponding to the flavor measurement can be written using Eq. (2) as,

$$F_l(\alpha) = \frac{(\partial_\alpha P_1(\alpha))^2}{P_1(\alpha)[1 - P_1(\alpha)]}, \quad (11)$$

where  $P_1(\alpha)$  is probability corresponding to any projector  $\hat{E}_1$ . However, for more general probability distributions involving multiple outcomes, the corresponding Fisher information must be computed using the full expression given in Eq. (2). The QFI is defined as the maximum of Fisher information calculated over all possible POVMs and satisfies,

$$F_l(\alpha) \leq F_Q(\alpha), \quad (12)$$

where the equality holds for optimal measurement strategies. Neutrino detection relies primarily on flavor identification via charged-current weak interactions, which effectively restricts the accessible measurements to the flavor basis. In contrast, for other quantum systems, more general measurement strategies can, in principle, be implemented to extract a larger amount of information from the underlying quantum state. It is also clear from above equation that flavor POVM corresponds to an experimentally realizable measurement, while the QFI is an ideal upper bound derived from neutrino state.

## III. METHODOLOGY

The LBL neutrino oscillation experiments NO $\nu$ A and T2K play a crucial role not only in addressing open questions within the standard three-neutrino framework but also in probing a variety of BSM physics scenarios [48–69]. These experiments operate at characteristic  $L/E$  values where oscillations driven by the atmospheric mass-squared difference dominate and accurate description of neutrino propagation requires matter effects taken into consideration. The evolution of an initial three-flavor state neutrino is governed by the effective Hamiltonian in matter,

$$H = \frac{1}{2E}U \text{diag}(0, \Delta m_{21}^2, \Delta m_{31}^2) U^\dagger + \text{diag}(V_{CC}, 0, 0), \quad (13)$$

where  $U$  is the PMNS matrix and  $V_{CC}$  is the matter potential. The matter potential is computed as:

$$V_{CC} = \sqrt{2}G_F n_e = 7.56 \times 10^{-14} \text{ eV} \cdot \rho [\text{g/cm}^3] \cdot Y_e, \quad (14)$$

where  $G_F$  is the Fermi constant and  $n_e$  is the electron number density.

The neutrino state evolution is obtained by  $|\nu(L)\rangle = e^{-iHL}|\nu(0)\rangle$ , where  $L$  is the propagation length. The appearance probability of  $\nu_\mu \rightarrow \nu_e$  can be given by  $P_{\mu e} = |\langle \nu_e | \nu(L) \rangle|^2$ . For antineutrinos, within the particle data group parameterization (PDG) of the leptonic mixing matrix [1], the CP phase transforms as  $\delta_{\text{CP}} \rightarrow -\delta_{\text{CP}}$  and the sign of matter potential will be flipped [70]. In our analysis, we consider the oscillation probability expressions in the approximation for constant matter density with  $\rho_{\text{NO}\nu A} = 2.8 \text{ g/cm}^3$ ,  $\rho_{\text{T2K}} = 2.6 \text{ g/cm}^3$ , and electron fraction  $Y_e = 0.5$ . The primary physics goals of current and future LBL experiments include the precise determination of  $\delta_{\text{CP}}$  and the resolution of the neutrino mass ordering [71–82], which is directly linked to the sign of the atmospheric mass squared splitting  $\Delta m_{31}^2$ .

Recently, studies based on quantum estimation theory have investigated the QFI associated with  $\delta_{\text{CP}}$  also within the single-parameter estimation framework and compared it with the Fisher information obtained from flavor POVMs, highlighting the role of flavor measurements in limiting the experimentally accessible CP information [23, 24, 26]. In this analysis, we do not separately consider the Fisher information associated with the flavor POVM, as in realistic experiments the oscillation probability at a specific energy is not directly observed. Instead, these oscillation probabilities are embedded in the reconstructed experimental event spectra, which include neutrino fluxes, interaction cross sections, and detector effects such as energy smearing, detector efficiencies, and backgrounds. Hence, the comparison between the event-level Fisher information and the event-weighted QFI benchmark provides a more reliable framework for understanding the experimentally accessible quantum information.

For a single neutrino, the QFI is given by Eq. (4). Let us now consider a LBL neutrino experiment with an expected number of events  $N_k(\delta_{\text{CP}})$  in the  $k$ -th energy bin. Using the additivity property of QFI, the corresponding QFI contribution per energy bin relevant for the detector can be approximated using Eq. (4) and Eq. (10) as

$$F_Q^{(k)}(\delta_{\text{CP}}) = N_k(\delta_{\text{CP}}) F_Q^{\text{pure}}(E_k, \delta_{\text{CP}}). \quad (15)$$

The total event-weighted QFI is then obtained by summing over all reconstructed energy bins,

$$F_Q^{\text{tot}}(\delta_{\text{CP}}) = \sum_k F_Q^{(k)}(\delta_{\text{CP}}). \quad (16)$$

Now to calculate the Fisher information at the event-level, we use standard statistics formalism [83]. Assuming statistically independent Poisson distributed events in each bin, the Fisher information associated with the parameter  $\delta_{\text{CP}}$  is given by,

$$F_{\text{event}}(\delta_{\text{CP}}) = \left\langle \left( \frac{\partial \ln \mathcal{L}}{\partial \delta_{\text{CP}}} \right)^2 \right\rangle, \quad (17)$$

where  $\mathcal{L}$  is the log-likelihood. Since the standard  $\chi^2$  function is  $\chi^2(\delta_{\text{CP}}) = -2 \ln \mathcal{L}$  then the Fisher information corresponds to the local curvature of the  $\chi^2$  function around the true values of parameter into consideration.

Using the general properties of Poisson statistics in Eq. (17), the event-level Fisher information per energy bin  $k$ , can be written as,

$$F_{\text{event}}^{(k)}(\delta_{\text{CP}}) = \frac{(\partial_{\delta_{\text{CP}}} N_k(\delta_{\text{CP}}))^2}{N_k(\delta_{\text{CP}})}, \quad (18)$$

and the total event-level Fisher information can be given by summing over all the energy bins,

$$F_{\text{event}}^{\text{tot}}(\delta_{\text{CP}}) = \sum_k F_{\text{event}}^{(k)}(\delta_{\text{CP}}). \quad (19)$$

Having established the event-level Fisher information formalism, in the next section, we now describe the experimental configurations relevant for this study, namely for NO $\nu$ A and T2K experiments.

#### IV. EXPERIMENTAL SETUP

In this section of the manuscript, we will focus on the description of the experimental configurations relevant for this study. Our analysis is specifically focused on the NO $\nu$ A and T2K experimental configurations, these LBL experiments operate at different baselines and energy regimes, thereby offering complementary sensitivities to oscillation parameters and potential new physics searches. In our simulations, we employ the GLOBES (General Long Baseline Experiment Simulator) software package [84, 85], which provides a comprehensive framework for simulating neutrino oscillation experiments including detector responses, neutrino fluxes, and systematic uncertainties. For each experiment, we employ the standard configuration files distributed within GLOBES, which were adapted to reproduce the nominal experimental setups as described in Refs. [7, 8]. These configurations contain experiment-specific parameters such as baseline lengths, target masses, neutrino fluxes, cross-sections, energy resolutions, and efficiencies. In the following subsections we detail the specific input parameters adopted for the NO $\nu$ A and T2K simulations, respectively.

##### A. T2K Experimental Configuration

The T2K experimental configuration provides a well-established framework for LBL neutrino oscillation studies, it employs a 295 km baseline from the J-PARC facility. In our analysis of the T2K setup we consider a fiducial target mass of 25 kt with a total exposure of 10 years, 4 years in neutrino mode and 6 years in antineutrino mode, driven by a beam power of 0.77 MW. Besides, the corresponding reconstructed events are selected within an energy range of 0.4 GeV to 1.2 GeV, binned into 20 equally distributed intervals. Furthermore, an energy resolution of 14% is assumed for both muon and electron channels. Here, the corresponding neutrino and antineutrino fluxes are normalized to 6.93 with a stored muon rate of  $10^{20}$  protons-on-target (POT) per year. In addition, the cross sections for charged-current (CC), neutral-current (NC), and quasi-elastic (QE) interactions are implemented as those given in GLOBES. In Table I we summarize the relevant parameters assumed in our simulation.

TABLE I. T2K experimental configuration parameters.

Parameter	Description	Value
$L$	Baseline length	295.0 km
$M_{\text{target}}$	Fiducial mass	25.0 kt
$t_\nu$	Neutrino running time	4 years
$t_{\bar{\nu}}$	Antineutrino running time	6 years
$P_{\text{beam}}$	Beam power	0.77 MW
$E_{\text{min}}$	Minimum reconstructed energy	0.4 GeV
$E_{\text{max}}$	Maximum reconstructed energy	1.2 GeV
$N_{\text{bins}}$	Number of energy bins	20
$\Delta E_\nu/E_\nu$	Energy resolution ( $\mu$ channel)	14%
$\Delta E_\nu/E_\nu$	Energy resolution ( $e$ channel)	14%

As far as background contaminants are concerned, the main background contributions arise from three sources. The first source of background is due to intrinsic  $\nu_e$  beam contamination, which is approximately 0.5% of the expected  $\nu_e$ -CC. The next source of contaminants consists of NC events misidentified as  $\nu_e$  interactions, contributing about 0.56%. The last source of background arises from  $\nu_\mu$ -CC events accompanied by  $\pi^0$  production, which represent a minor fraction of about 0.03%. In addition to the corresponding backgrounds, we also include systematic uncertainties. These are parameterized by a spectrum tilt following Ref. [86], the normalization errors are set to 5% for charged current appearance events and 20% for the aforementioned backgrounds. In Table II we present the corresponding efficiencies and normalization uncertainties for the expected signal events, quasi-elastic and charged-current interactions, considered in our simulation of the T2K configuration.

TABLE II. T2K signal channels and systematic uncertainties.

Channel	Signal Efficiency	Normalization Error
$\nu_\mu \rightarrow \nu_e$ (QE)	50.5%	10%
$\bar{\nu}_\mu \rightarrow \bar{\nu}_e$ (QE)	50.5%	10%
$\nu_\mu \rightarrow \nu_\mu$ (QE)	90%	2.5%
$\bar{\nu}_\mu \rightarrow \bar{\nu}_\mu$ (QE)	90%	2.5%
$\nu_\mu \rightarrow \nu_e$ (CC)	50.5%	5%
$\bar{\nu}_\mu \rightarrow \bar{\nu}_e$ (CC)	50.5%	5%

## B. NO $\nu$ A Experimental Configuration

The NO $\nu$ A experiment features a longer baseline of 812 km from Fermilab to a 14 kt detector in Ash River, Minnesota. In this analysis, we consider a fiducial target mass of 25 kt with a total exposure of 10 years, 5 years in neutrino mode and 5 years in antineutrino mode, driven by a beam power of 1.12 MW. Besides, the reconstructed events are selected within an energy range of 1.0 GeV to 3.5 GeV, binned into 20 equally-distributed intervals. An energy resolution of 16% is assumed for the muon channel and 14% for the electron channel, reflecting the different reconstruction performances for each topology. The fluxes

for this configuration are properly normalized to  $6.48 \times 10^{-19}$  with a stored muon rate of  $10^{20}$  POT per-year. In Table III we display the corresponding parameters considered in our simulation of the NO $\nu$ A configuration.

TABLE III. NO $\nu$ A experimental configuration parameters.

Parameter	Description	Value
$L$	Baseline length	812.0 km
$M_{\text{target}}$	Fiducial mass	25.0 kt
$t_\nu, t_{\bar{\nu}}$	Running time (each)	5 years
$P_{\text{beam}}$	Beam power	1.12 MW
$E_{\text{min}}$	Minimum reconstructed energy	1.0 GeV
$E_{\text{max}}$	Maximum reconstructed energy	3.5 GeV
$N_{\text{bins}}$	Number of energy bins	20
$\Delta E_\nu/E_\nu$	Energy resolution ( $\mu$ channel)	16%
$\Delta E_\nu/E_\nu$	Energy resolution ( $e$ channel)	14%

The background budget comprises three main contributions, the largest of which arises from the intrinsic  $\nu_e$  beam contamination, which accounts for 12.0% of the  $\nu_e$ -CC events. Moreover, misidentified  $\nu_\mu$ -NC events with  $\pi^0$  production contribute 0.15%, while the charged-current  $\nu_\mu$  misidentification events represent a smaller fraction of about 0.04%. For all channels, a uniform normalization uncertainty of 5% is assumed, including both signal and background events. In Table IV we present the corresponding efficiencies and normalization uncertainties for the expected signal channels adopted in our simulation of the NO $\nu$ A setup.

TABLE IV. NO $\nu$ A signal channels and systematic uncertainties.

Channel	Signal Efficiency	Normalization Error
$\nu_\mu \rightarrow \nu_e$ (CC)	24%	5%
$\nu_\mu \rightarrow \nu_\mu$ (CC)	80%	5%
$\bar{\nu}_\mu \rightarrow \bar{\nu}_e$ (CC)	37%	5%
$\bar{\nu}_\mu \rightarrow \bar{\nu}_\mu$ (CC)	80%	5%

### C. Expected event rates computation

The oscillation probabilities are computed including matter effects under the constant density approximation. In our simulations, we adopt the best-fit values of the neutrino oscillation parameters from Ref. [87], which are summarized in Table V. In the following discussions, NO and IO denote normal ordering and inverted ordering, respectively. Besides, the expected number of events in energy bin  $k$  for a given channel is computed as:

$$N_k(\delta_{\text{CP}}) = \int_{E_\nu^{\text{min}}}^{E_\nu^{\text{max}}} \Phi(E_\nu) \sigma(E_\nu) P_{\mu e}(E_\nu, \delta_{\text{CP}}) \epsilon(E_\nu) R(E_\nu, E_k) dE_\nu, \quad (20)$$

where  $\Phi(E_\nu)$  is the neutrino flux,  $\sigma(E_\nu)$  is the interaction cross section,  $P_{\mu e}(E_\nu, \delta_{\text{CP}})$  is the oscillation probability including matter effects,  $\epsilon(E_\nu)$  is the detection efficiency, and  $R(E_\nu, E_k)$  is the energy resolution function, modeled as Gaussian smearing with width  $\sigma(E_\nu)$  taken from Table I for T2K or Table III for NO $\nu$ A.

TABLE V. Corresponding neutrino oscillation parameters considered in this study.

Neutrino Oscillation Parameter	Best-fit value
$\theta_{12}$	$33.44^\circ$
$\theta_{13}$	$8.57^\circ$
$\theta_{23}$	$49.2^\circ$
$\Delta m_{21}^2$	$7.42 \times 10^{-5} \text{ eV}^2$
$\Delta m_{31}^2$ (NO)	$+2.517 \times 10^{-3} \text{ eV}^2$
$\Delta m_{31}^2$ (IO)	$-2.498 \times 10^{-3} \text{ eV}^2$

In Table VI, we summarize the total (simulated) expected event rates against the published results from the T2K and NO $\nu$ A collaborations, including both appearance and disappearance channels. These rates correspond to the combined contributions from neutrino and antineutrino polarities. For each experimental configuration and each value of  $\delta_{\text{CP}}$  displayed, the comparison between our simulation and the measured events leads to differences below 5%.

TABLE VI. Total (appearance plus disappearance) expected event rates.

Experiment	$\delta_{\text{CP}}$	Our Simulation	Reference	Difference
T2K (NO)	0	$78.4 \pm 8.9$	$75.3 \pm 9.2$ [7]	4.1%
T2K (NO)	$\pi$	$124.2 \pm 11.1$	$118.7 \pm 10.8$ [7]	4.6%
NO $\nu$ A (NO)	0	$42.3 \pm 5.1$	$40.8 \pm 5.5$ [8]	3.7%
NO $\nu$ A (NO)	$\pi$	$28.7 \pm 4.2$	$27.9 \pm 4.5$ [8]	2.9%

## V. RESULTS AND DISCUSSIONS

Accelerator-based LBL experiments provide a controlled source of neutrinos and can operate in both neutrino and antineutrino beam modes. Since neutrinos and antineutrinos interact differently with the Earth's matter during propagation, the corresponding oscillation probabilities are modified differently by matter effects. Therefore, in order to isolate genuine leptonic CP-violating effects from matter-induced asymmetries, precise measurements of the  $\nu_\mu \rightarrow \nu_e$  and  $\bar{\nu}_\mu \rightarrow \bar{\nu}_e$  appearance channels as a function of energy are required.

The evolution of neutrino and antineutrino states differs at the fundamental level due to the opposite sign of the matter potential and the transformation  $\delta_{\text{CP}} \rightarrow -\delta_{\text{CP}}$ . Consequently, the QFI associated with  $\delta_{\text{CP}}$  is expected to differ between neutrino and antineutrino modes, as well as for NO and IO. Since the expected event spectra and statistics are different for NO $\nu$ A and T2K in both beam modes, it is important to analyze the neutrino and antineutrino channels separately in the subsequent discussion.

### A. QFI for neutrino and antineutrino state

In Fig.1, we demonstrate the behavior of QFI for the leptonic CP violating phase as a function of energy for T2K and NO $\nu$ A for both states i.e. neutrino and antineutrino. The QFI associated with both states shows a broader maxima around the first oscillation maximum and gradually decreases with the increase in energy for both T2K and NO $\nu$ A. We show the values of QFI for  $\delta_{CP} = -\pi/2, 0, \pi/2$ , and the dependence on the  $\delta_{CP}$  is evident to be weaker indicating that the change in the neutrino state associated with the change in the CP phase remains nearly stable.

On the other hand, an asymmetry is observed between the neutrino and antineutrino state if we change the neutrino mass ordering due to the sign flip of the matter potential for neutrino and antineutrino evolution in matter. The observed QFI is larger in the neutrino state for NO as compared to the antineutrino state in the same ordering. For IO, the QFI is found to be larger in magnitude for antineutrino than the neutrino state. We observe the same behavior in both T2K and NO $\nu$ A, but the difference is evident to be larger in NO $\nu$ A, owing to the strong matter effects due to longer baseline.

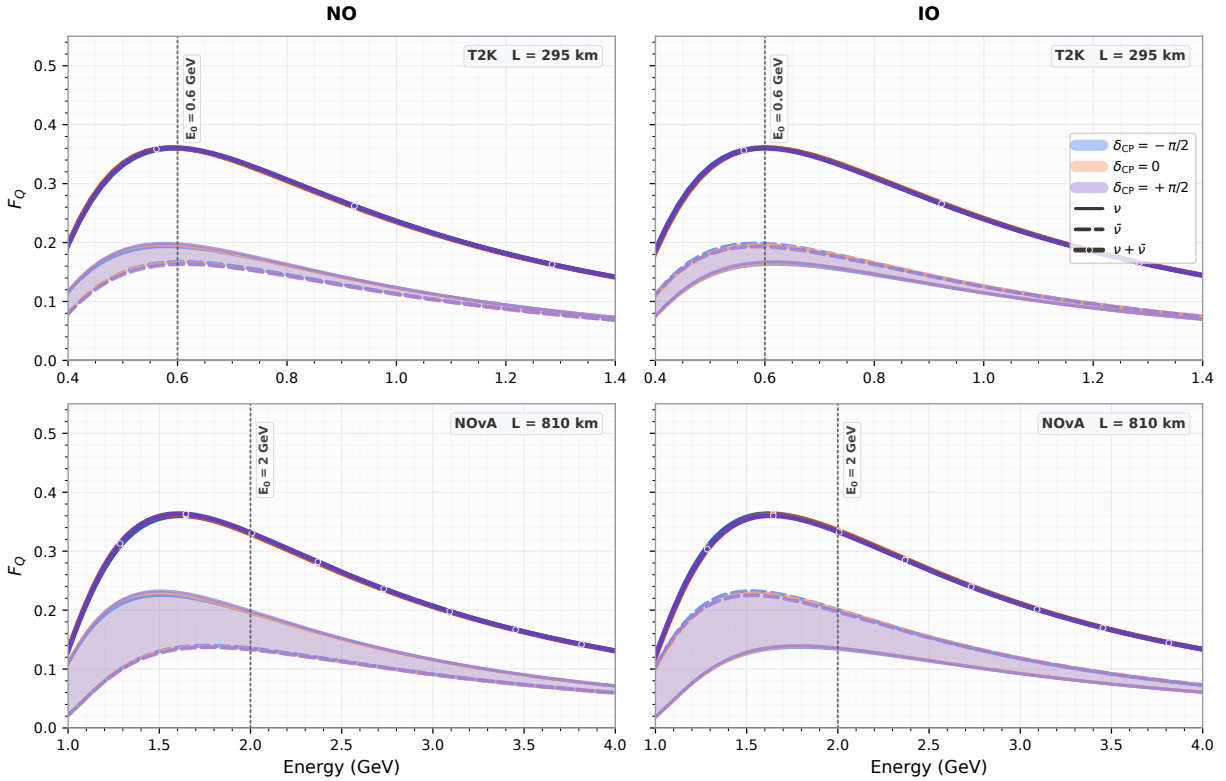


FIG. 1. QFI associated with  $\delta_{CP}$  as a function of neutrino energy for T2K and NO $\nu$ A for both neutrino and antineutrino states. The left panel corresponds to NO, while the right panel shows the results for IO. Vertical dashed lines denote flux peak energies. See the text for a detailed explanation.

This result suggests that the amount of information encoded about the parameter  $\delta_{CP}$ , is intrinsically different for neutrino and antineutrino quantum state. This feature vanishes when we combine both states and the resultant combined QFI is same for both NO and IO

and is almost independent of the chosen values of  $\delta_{\text{CP}}$ . The magnitude also remains same for T2K and NO $\nu$ A both, as the matter effects also gets canceled in the combination of both states. Hence, it becomes important to consider the neutrino and antineutrino mode separately in the analysis, since the corresponding event spectra in these LBL experiments differ significantly. This also makes the comparison between the QFI and the event-level Fisher information particularly relevant for understanding the CP sensitivity of T2K and NO $\nu$ A from information perspective.

To further investigate the disparity in QFI for NO and IO shown in Fig. 1, we define an asymmetry,  $A_{\text{QFI}}$ , between the calculated values of QFI in neutrino and antineutrino state which measures the relative difference between them:

$$A_{\text{QFI}} = \frac{F_Q^\nu - F_Q^{\bar{\nu}}}{F_Q^\nu + F_Q^{\bar{\nu}}}, \quad (21)$$

where  $F_Q^\nu$  and  $F_Q^{\bar{\nu}}$  corresponds to the QFI associated with neutrino and antineutrino state, respectively. Furthermore, to gain more insights into the behavior of  $A_{\text{QFI}}$ , we also consider the probability asymmetry, defined as,

$$A_{\text{CP}} = \frac{P(\nu_\mu \rightarrow \nu_e) - P(\bar{\nu}_\mu \rightarrow \bar{\nu}_e)}{P(\nu_\mu \rightarrow \nu_e) + P(\bar{\nu}_\mu \rightarrow \bar{\nu}_e)}. \quad (22)$$

While  $A_{\text{CP}}$  characterizes the magnitude and sign of CP violation at the oscillation probability level,  $A_{\text{QFI}}$  quantifies the relative amount of quantum information about the CP-violating phase  $\delta_{\text{CP}}$  carried by neutrino and antineutrino states. In Fig. 2, we show the probability asymmetry  $A_{\text{CP}}$  and the QFI asymmetry  $A_{\text{QFI}}$  as functions of neutrino energy for the T2K (upper panels) and NO $\nu$ A (lower panels) configurations at three representative values of the Dirac CP phase,  $\delta_{\text{CP}} = -\pi/2, 0, \pi/2$ .

For the NO scenario in NO $\nu$ A, both asymmetries,  $A_{\text{CP}}$  and  $A_{\text{QFI}}$ , remain positive over the considered energy range for all benchmark values of  $\delta_{\text{CP}}$  as the matter potential enhances  $\nu_\mu \rightarrow \nu_e$  transition probability. In contrast, for IO, the asymmetries exhibit the opposite behavior as the corresponding antineutrino channel is enhanced due to matter effects. This behavior indicates the matter enhancement in the probabilities is ordering dependent. The same behavior is also observed for QFI asymmetry between both quantum states.

For the T2K configuration with NO, both asymmetries are also predominantly positive, except for the case  $\delta_{\text{CP}} = +\pi/2$  (purple solid curve). On the other hand, in the IO scenario, both asymmetries become negative over most of the energy range, except for the case  $\delta_{\text{CP}} = -\pi/2$  (blue solid curve). The variation in the sign of the asymmetries in T2K arises from the combined effect of CP violation and matter effects in neutrino and antineutrino propagation. The behavior of  $A_{\text{QFI}}$  demonstrates that the intrinsic quantum sensitivity to  $\delta_{\text{CP}}$  already contains a hierarchy-dependent asymmetry between neutrino and antineutrino propagation.

Despite the clear sensitivity of  $A_{\text{QFI}}$  to the neutrino mass ordering for both T2K and NO $\nu$ A, its dependence on the value of  $\delta_{\text{CP}}$  remains relatively weak within a given ordering. This indicates that although the QFI asymmetry efficiently captures the hierarchy-dependent differences between neutrino and antineutrino propagation, it is comparatively less sensitive to variations in the CP phase itself. It should also be noted that a large probability asymmetry may also imply a significant variation in the intrinsic quantum sensitivity encoded in the propagated neutrino state.

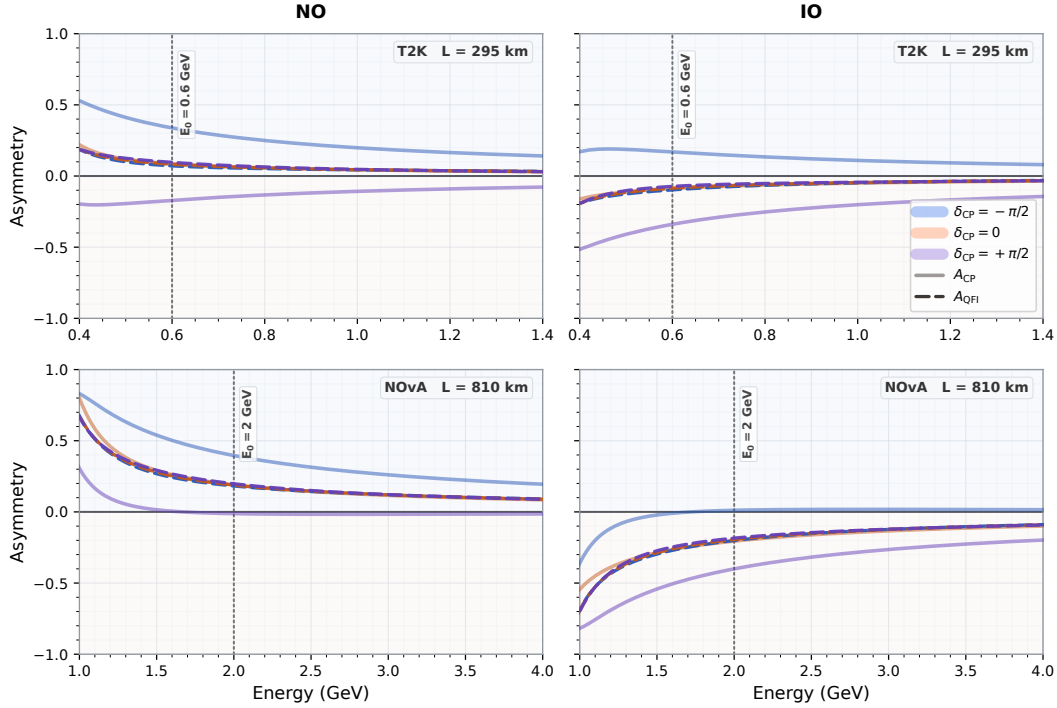


FIG. 2. The probability asymmetry  $A_{CP}$  (solid) and QFI asymmetry  $A_{QFI}$  (dashed) as a function of the neutrino energy for T2K (upper panels) and NO $\nu$ A (lower panels) setups. The left panels consider the case of NO while right panels represent the IO scenario. See the text for a detailed explanation.

It is important to emphasize that the QFI itself is not a directly experimentally observable quantity, but rather represents the ultimate quantum limit on parameter estimation achievable over all possible measurements. In LBL experiments, the experimentally accessible observables are reconstructed neutrino and antineutrino event spectra, which involve different event statistics. Therefore, using the additivity property of QFI, the relevant comparison is between the event-level Fisher information and the event-weighted QFI benchmark, rather than the intrinsic single-neutrino QFI itself. Motivated by this observation, in the following subsections we investigate the detector-level extraction of CP information through the event-weighted QFI and the corresponding event-level Fisher information constructed from neutrino spectra.

## B. Neutrino Appearance Channel at T2K and NO $\nu$ A

In Fig. 3, we present the expected neutrino and antineutrino appearance event spectra for the T2K experimental configuration. The event rates are evaluated at  $\delta_{CP} = 0$ ,  $-\pi/2$ , and  $\pi/2$ , providing a comprehensive comparison between CP-conserving and CP-violating phase values. For both neutrino and antineutrino modes, the event spectrum peaks near 0.7 GeV, consistent with the flux maximum at the 295 km baseline in T2K. The spectral separation is notable between the  $\delta_{CP} = 0$  (green lines) and  $\delta_{CP} = \pm\pi/2$  (red/blue lines)

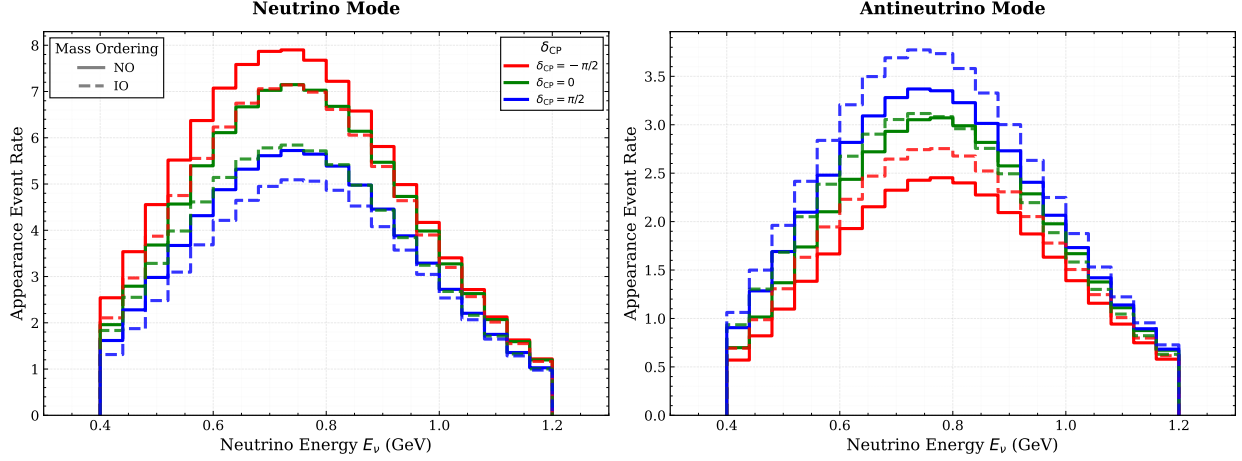


FIG. 3. Expected  $\nu_e$  (solid lines) and  $\bar{\nu}_e$  (dashed lines) appearance event spectra for the T2K configuration, evaluated at three representative values of  $\delta_{\text{CP}}$  ( $0$ ,  $-\pi/2$ , and  $\pi/2$ ). The spectra correspond to a total exposure of 4 years in neutrino mode and 6 years in antineutrino mode with a 0.77 MW beam, accumulated within the reconstructed energy range of 0.4 to 1.2 GeV. See the text for a detailed explanation.

values, in both neutrino and antineutrino channels, illustrating the sensitivity of the T2K experiment to leptonic CP violation.

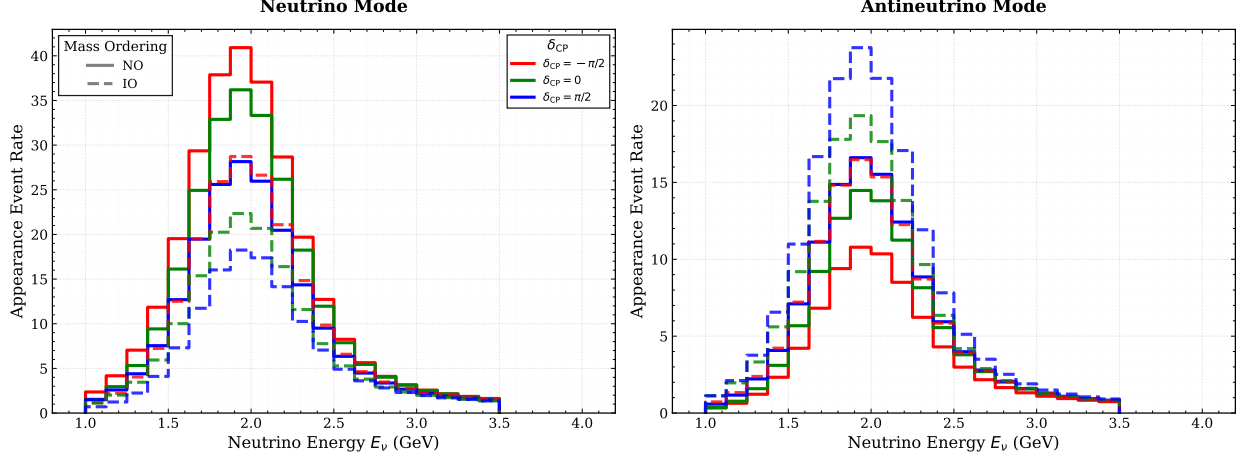


FIG. 4. Expected  $\nu_e$  (solid lines) and  $\bar{\nu}_e$  (dashed lines) appearance event spectra for the  $\text{NO}\nu\text{A}$  configuration, evaluated at three representative values of  $\delta_{\text{CP}}$  ( $0$ ,  $-\pi/2$ , and  $\pi/2$ ). The spectra correspond to a total exposure of 5 years in neutrino mode and 5 years in antineutrino mode with a 1.12 MW beam, accumulated within the energy window of 1.0 to 3.5 GeV. See the text for a detailed explanation.

In Fig. 4, we display the expected neutrino and antineutrino appearance events for the  $\text{NO}\nu\text{A}$  configuration. The event distributions are evaluated at three benchmark values of the CP-violating phase:  $\delta_{\text{CP}} = 0$ ,  $-\pi/2$ , and  $\pi/2$ , including both CP-conserving and CP-violating values. The corresponding spectral peak around 2 GeV is consistent with the oscillation maximum for the 812 km baseline at  $\text{NO}\nu\text{A}$ . For instance, a distinct separation

is observed between the  $\delta_{\text{CP}} = 0$  and  $\delta_{\text{CP}} = \pm\pi/2$  spectra in both neutrino and antineutrino modes, reflecting the sensitivity of the  $\text{NO}\nu\text{A}$  configuration to the CP-violating phase through the appearance channel.

The information relevant for the estimation of the leptonic CP phase is fundamentally encoded in the reconstructed spectral information of these experiments. The dependence of the event spectra shown in Fig. 3 and Fig. 4 on  $\delta_{\text{CP}}$  originates directly from the underlying oscillation probabilities. The spectral separation between different  $\delta_{\text{CP}}$  hypotheses becomes more pronounced near the first oscillation maximum, where the CP-sensitive interference terms are significant. Furthermore, since the matter potential enters with opposite sign for neutrino and antineutrino propagation, distinct differences are observed between the two beam modes for both NO and IO. These effects are more prominent in  $\text{NO}\nu\text{A}$  because of its longer baseline and consequently stronger matter effects compared to T2K.

### C. Event-weighted Quantum Fisher Information

The QFI discussed in the previous subsection represents the intrinsic quantum sensitivity associated with a single evolved neutrino state. In the following analysis, we instead consider the event-weighted QFI defined in Eq. (15). This quantity serves as an effective benchmark for the intrinsic quantum sensitivity of neutrino oscillation states while simultaneously incorporating the event-level statistical information accessible in the experiments.

In Fig. 5, we show the event-weighted QFI as a function of neutrino energy  $E_\nu$  and the leptonic CP phase  $\delta_{\text{CP}}$  for the T2K configuration. The left and right panels correspond to the neutrino and antineutrino modes, respectively, while the upper and lower panels assume NO and IO. The event-weighted QFI in the neutrino mode remains comparatively larger than that in the antineutrino mode for both orderings due to larger statistics, with the dominant region appearing near  $\delta_{\text{CP}} = -\pi/2$ . The relatively weak variation between NO and IO originates from the shorter baseline of T2K and consequently smaller matter effects, leading to a reduced neutrino-antineutrino asymmetry in the event-weighted QFI distribution.

In Fig. 6, we present the corresponding event-weighted QFI distributions for the  $\text{NO}\nu\text{A}$  configuration. The left panels correspond to the neutrino mode, while the right panels show the antineutrino mode. The upper and lower panels assume NO and IO, respectively. In contrast to T2K, a stronger hierarchy-dependent asymmetry is observed due to the larger matter effects at the longer  $\text{NO}\nu\text{A}$  baseline. For NO, the event-weighted QFI is significantly enhanced in the neutrino mode compared to the antineutrino mode, with the largest concentration appearing near  $\delta_{\text{CP}} = -\pi/2$ . On the other hand, for inverted ordering, the antineutrino mode becomes comparatively more enhanced, with the dominant region shifting toward  $\delta_{\text{CP}} = +\pi/2$ . This behavior reflects the hierarchy-dependent matter enhancement in  $\text{NO}\nu\text{A}$ , where matter effects preferentially enhance the  $\nu_\mu \rightarrow \nu_e$  channel for NO and the  $\bar{\nu}_\mu \rightarrow \bar{\nu}_e$  channel for IO, thereby redistributing the experimentally relevant CP information between neutrino and antineutrino modes.

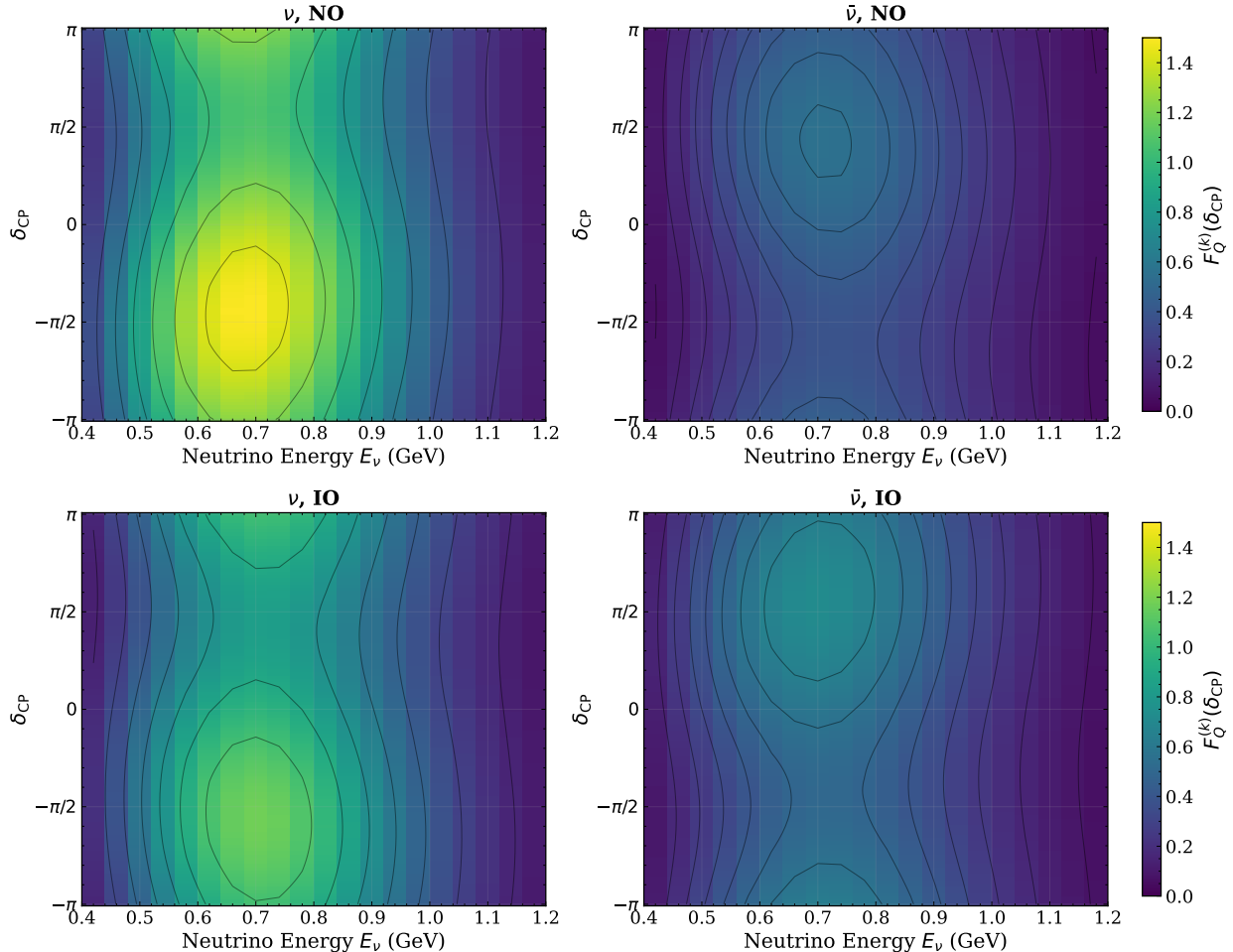


FIG. 5. Event-weighted QFI  $F_Q^{(k)}(\delta_{CP})$  as a function of the neutrino energy  $E_\nu$  and the leptonic CP-violating phase  $\delta_{CP}$  for the T2K setup. The left panels correspond to the neutrino mode, while the right panels show the antineutrino mode. The upper and lower panels assume NO and IO, respectively. See the text for a detailed explanation.

Although the intrinsic single-state QFI remains relatively similar between the two mass orderings, the event-weighted QFI exhibits noticeably different structures once event statistics are included. In particular, for the NO $\nu$ A experiment, the event-weighted QFI exhibits a comparatively more concentrated structure, while for T2K the accessible CP information is distributed more broadly across the  $(E_\nu, \delta_{CP})$  parameter space. Unlike the intrinsic single-state QFI discussed previously, which showed only a relatively weak dependence on  $\delta_{CP}$ , the inclusion of event statistics through the additivity property of QFI introduces a significantly stronger  $\delta_{CP}$  dependence in the experimentally relevant information landscape. This demonstrates that the interplay between event statistics and matter effects can substantially reshape the accessible quantum-information structure compared to the intrinsic single-state sensitivity alone.

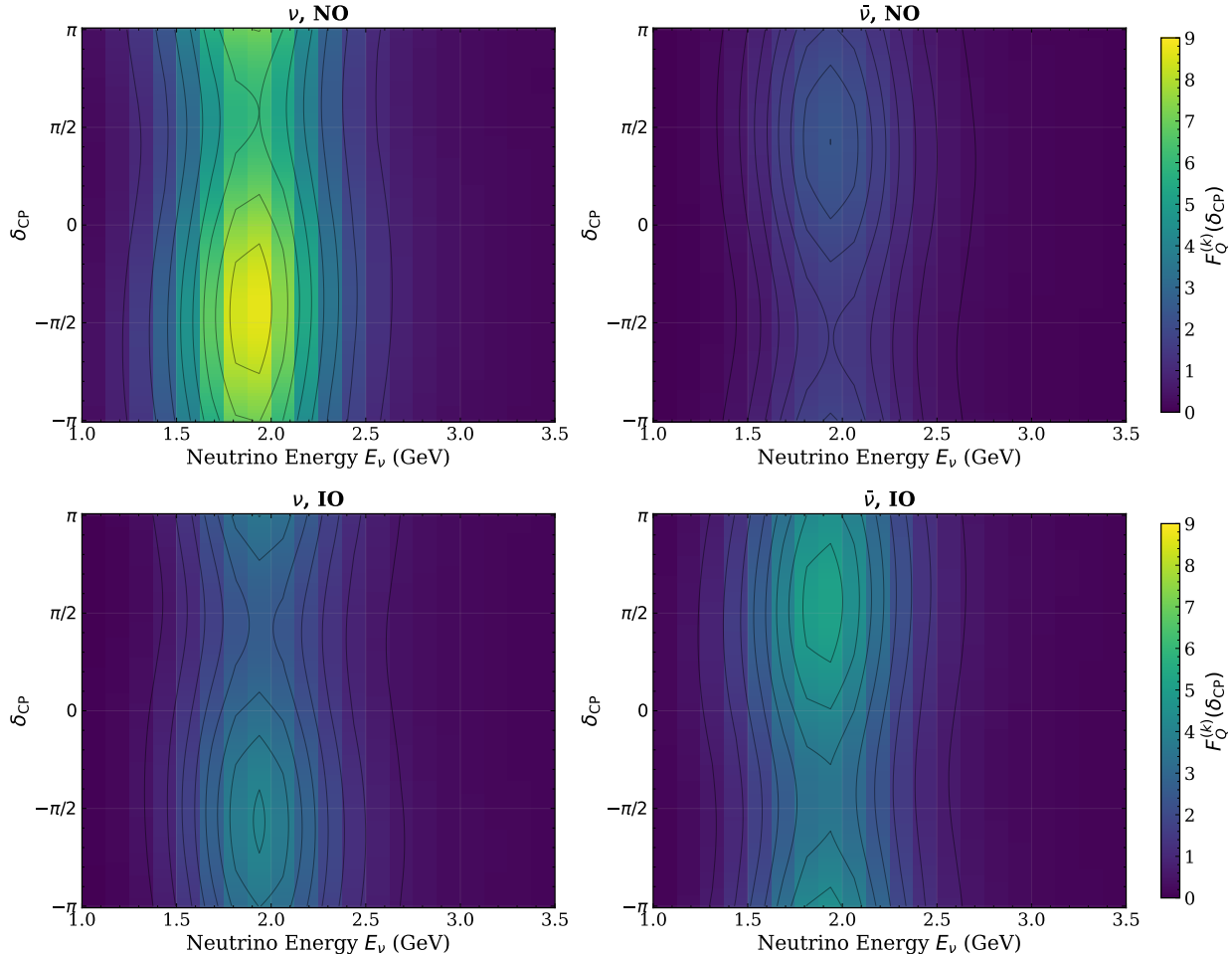


FIG. 6. Event-weighted QFI  $F_Q^{(k)}(\delta_{CP})$  as a function of the neutrino energy  $E_\nu$  and the leptonic CP-violating phase  $\delta_{CP}$  for the  $\text{NO}\nu A$  configuration. The left panels correspond to the neutrino mode, while the right panels show the antineutrino mode. The upper and lower panels assume NO and IO, accordingly. See the text for a detailed explanation.

#### D. Event-level Fisher Information

The experimentally accessible sensitivity to  $\delta_{CP}$  is governed by the variation of the reconstructed event spectra with respect to the CP phase. The corresponding change in the expected number of events in each reconstructed energy bin can be written using Eq. (20) as,

$$\frac{\partial N_k}{\partial \delta_{CP}} = \int dE_\nu \Phi(E_\nu) \sigma(E_\nu) \epsilon(E_\nu) R(E_\nu, E_k) \frac{\partial P_{\mu e}(E_\nu, \delta_{CP})}{\partial \delta_{CP}}. \quad (23)$$

This quantity can be used directly to determine the event-level Fisher information associated with the event spectra per energy bin. Similar to the flavor POVM Fisher information, the experimentally accessible sensitivity is ultimately governed by the variation of the oscillation probability with respect to  $\delta_{CP}$ . However, in experiments this information is embedded within reconstructed event spectra after including flux, cross-section, and detector response. Hence, by using the quantity from Eq. (23) in Eq. (18), the event-level Fisher information

associated with the experimentally reconstructed spectra can be obtained.

Fig. 7 presents the event-level Fisher information distributions for the T2K configuration. The dominant information region ( $F_{\text{event}}(E_\nu, \delta_{\text{CP}}) \sim 0.2$ ) appears near the first oscillation maximum around  $E_\nu \sim 0.6$  GeV and close to the CP-conserving phases  $\delta_{\text{CP}} = 0$  and  $\pm\pi$ . Due to the shorter baseline and consequently weaker matter effects, the neutrino and antineutrino modes exhibit comparatively similar overall structures with lower values of  $F_{\text{event}}(E_\nu, \delta_{\text{CP}})$  for the case of antineutrino mode due to lower statistics, although the contour tilts are reversed between the two beam modes. This opposite tilt originates from the CP-conjugate interference structure in the oscillation probabilities through the replacement  $\delta_{\text{CP}} \rightarrow -\delta_{\text{CP}}$  for antineutrinos.

The distinction between NO and IO remains relatively weak in both magnitude and overall distribution, reflecting the limited hierarchy sensitivity of T2K. The event-level Fisher information is minimized near the maximally CP-violating values  $\delta_{\text{CP}} = \pm\pi/2$ , where the local variation of the reconstructed spectra with respect to  $\delta_{\text{CP}}$  becomes comparatively weaker. Compared to the corresponding event-weighted QFI distributions in Fig. 5, the event-level Fisher information remains smaller, reflecting the information loss associated with the flavor measurement scheme.

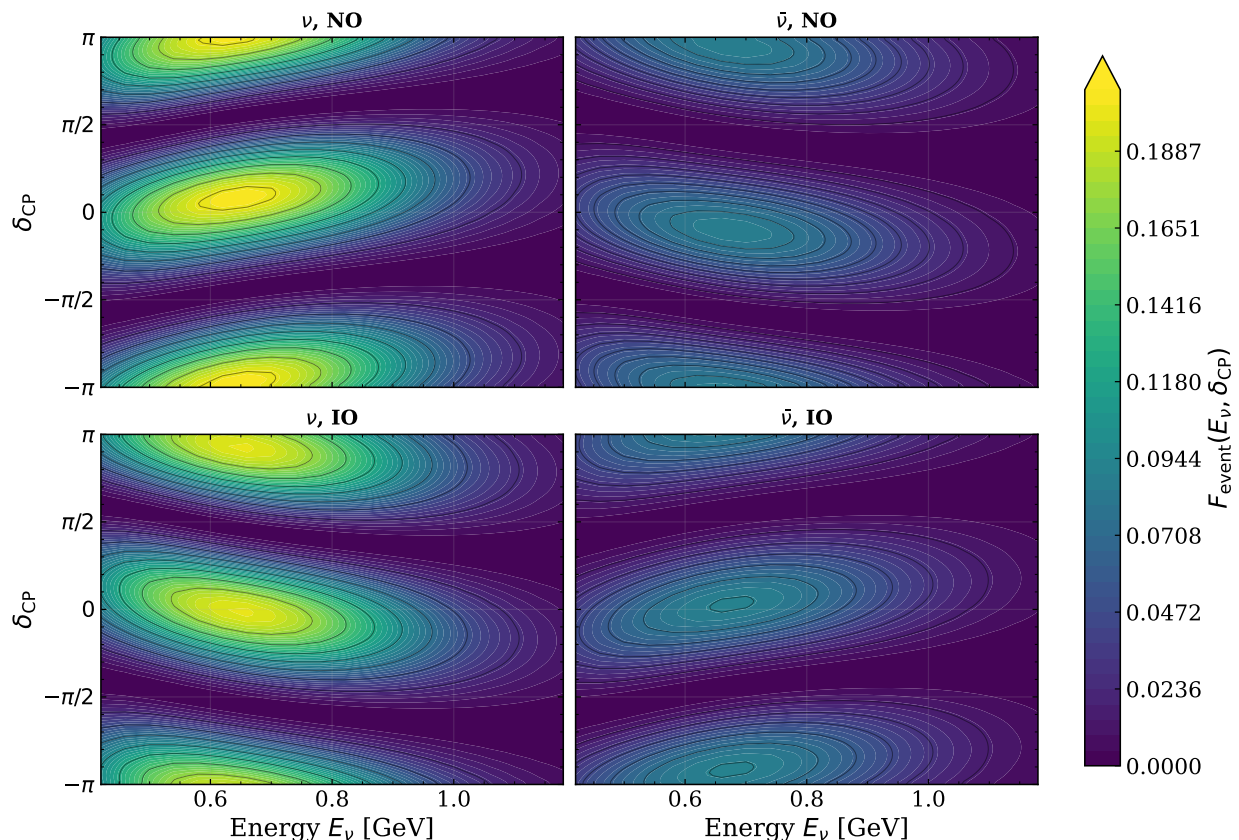


FIG. 7. Event-level Fisher information  $F_{\text{event}}(E_\nu, \delta_{\text{CP}})$  for the T2K configuration. The color scale represents the Fisher information contribution per reconstructed energy bin as a function of  $\delta_{\text{CP}}$  (vertical axis) and neutrino energy  $E_\nu$  (horizontal axis). The left (right) panels show the neutrino (antineutrino) mode, while the upper (lower) rows assume NO (IO). See the text for a detailed explanation.

Fig. 8 shows the corresponding event-level Fisher information distributions for the  $\text{NO}\nu\text{A}$  configuration. For both orderings, the neutrino mode exhibits the dominant information region ( $F_{\text{event}}(E_\nu, \delta_{\text{CP}}) \sim 1.2$ ) near the first oscillation maximum around  $E_\nu \sim 2$  GeV, particularly close to the CP-conserving phases  $\delta_{\text{CP}} = 0$  and  $\pm\pi$ , while the antineutrino mode carries comparatively smaller information. Unlike the T2K configuration,  $\text{NO}\nu\text{A}$  exhibits a comparatively narrower information distribution due to its stronger matter effects and more localized energy spectrum. Furthermore, the event-level Fisher information  $F_{\text{event}}(E_\nu, \delta_{\text{CP}})$  shows no strong hierarchy dependence in the overall contour structure for both neutrino and antineutrino modes, although the relative magnitude of the information content is redistributed between the two beam modes.

Thus, we observe that the event-level Fisher information as shown in Figs. 7 and 8 does not fully saturate the corresponding event-weighted QFI as in Figs. 5 and 6. Therefore, the comparison between these two quantities becomes important for analyzing the efficiency of these experiments in extracting the information available for the estimation of the parameter under consideration.

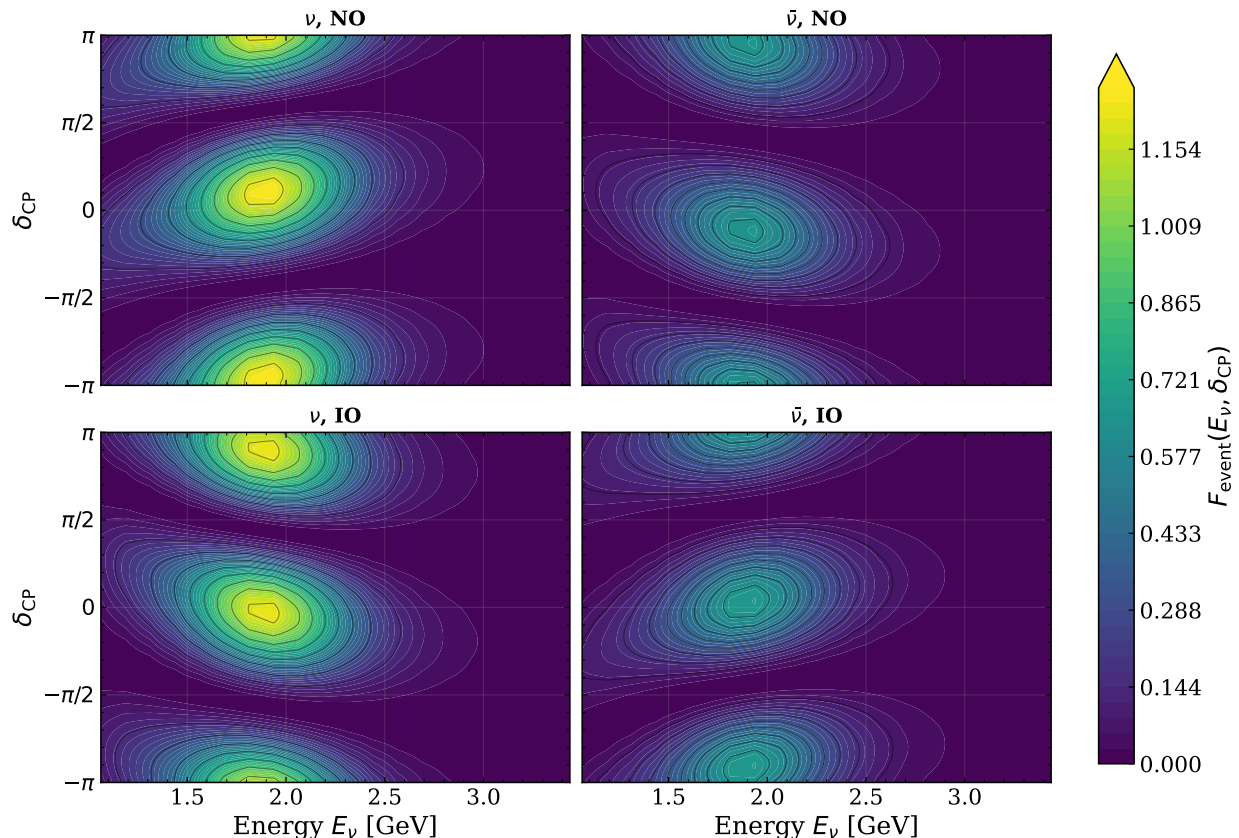


FIG. 8. Event-level Fisher information  $F_{\text{event}}(E_\nu, \delta_{\text{CP}})$  for the  $\text{NO}\nu\text{A}$  configuration. The color scale represents the Fisher information contribution per reconstructed energy bin as a function of the CP-violating phase  $\delta_{\text{CP}}$  (vertical axis) and neutrino energy  $E_\nu$  (horizontal axis). The left (right) panels show the neutrino (antineutrino) mode, while the upper (lower) rows assume NO (IO). See the text for a detailed explanation

### E. Experimental Extraction Efficiency

Hence, in order to quantify how efficiently the experimentally reconstructed spectra extract the available quantum information associated with  $\delta_{\text{CP}}$ , we define a ratio:

$$\eta_{\text{event}}^{(k)}(\delta_{\text{CP}}) = \frac{F_{\text{event}}^{(k)}(\delta_{\text{CP}})}{F_Q^{(k)}(\delta_{\text{CP}})}, \quad (24)$$

In Fig. 9 we show the behavior of bin-wise extraction efficiency in as a function of neutrino energy  $E_\nu$  (horizontal axis) and the leptonic CP phase  $\delta_{\text{CP}}$  (vertical axis) for both the T2K and NO $\nu$ A configurations. The brighter regions in the contour represent the ranges of energy and CP phase where the amount of extracted information from the effective event-weighted QFI in the detectors is maximal, while the darker regions correspond to limited extraction efficiency. For T2K, the extraction efficiency remains moderate, around 0.3, over a broader energy range. This behavior follows a similar pattern to that of  $F_{\text{event}}^{(k)}$  for both neutrino and antineutrino modes and shows weak hierarchy dependence between the two mass orderings. It is evident from the figure that around  $\delta_{\text{CP}} = \pm\pi/2$ , the extraction efficiency becomes very low irrespective of the presence of information in the quantum state.

For NO $\nu$ A, the extraction efficiency reaches values close to  $\sim 0.9$  at lower energies. The overall structure of the distribution is comparatively less broad than that of T2K, and the dependence on the neutrino mass ordering is more pronounced. For NO, the antineutrino mode shows comparatively larger extraction efficiency than the neutrino mode, while for IO this behavior reverses. At lower energies, NO $\nu$ A exhibits better extraction efficiency near the CP-violating values of  $\delta_{\text{CP}}$ . However, as the energy increases, the extraction efficiency gradually decreases toward smaller values.

In Fig. 10 we present the total extraction efficiency, defined as,

$$\eta_{\text{event}}^{\text{tot}}(\delta_{\text{CP}}) = \frac{F_{\text{event}}^{\text{tot}}(\delta_{\text{CP}})}{F_Q^{\text{tot}}(\delta_{\text{CP}})}, \quad (25)$$

for the T2K (blue) and NO $\nu$ A (red) experimental setups. In both experiments, the solid, dashed, and dot-dashed lines correspond to the neutrino mode, antineutrino mode, and the combination of both modes, respectively. It is evident from the figure that for both experiments, the total extraction efficiency remains significantly below the event-weighted quantum benchmark for both beam modes. This shows that these experiments do not fully access the intrinsic quantum information available in the neutrino state for the estimation of  $\delta_{\text{CP}}$ .

For the case of the NO $\nu$ A under IO, the total extraction efficiency is slightly larger than that of T2K for most of the  $\delta_{\text{CP}}$  values while for NO it remains almost similar. This trend is partially due to the fact that the NO $\nu$ A configuration experiences larger matter effects and enhanced flavor asymmetry as compared to T2K, as we discussed in Section V A. It is to be noted that the extraction efficiency is decreases significantly around the maximal CP-violating values of the CP phase i.e.  $\delta_{\text{CP}} \simeq \pm\pi/2$  for both experiments and all beam modes, indicating that event spectra become locally less distinguishable under small CP-phase variations regardless of the intrinsic quantum information.

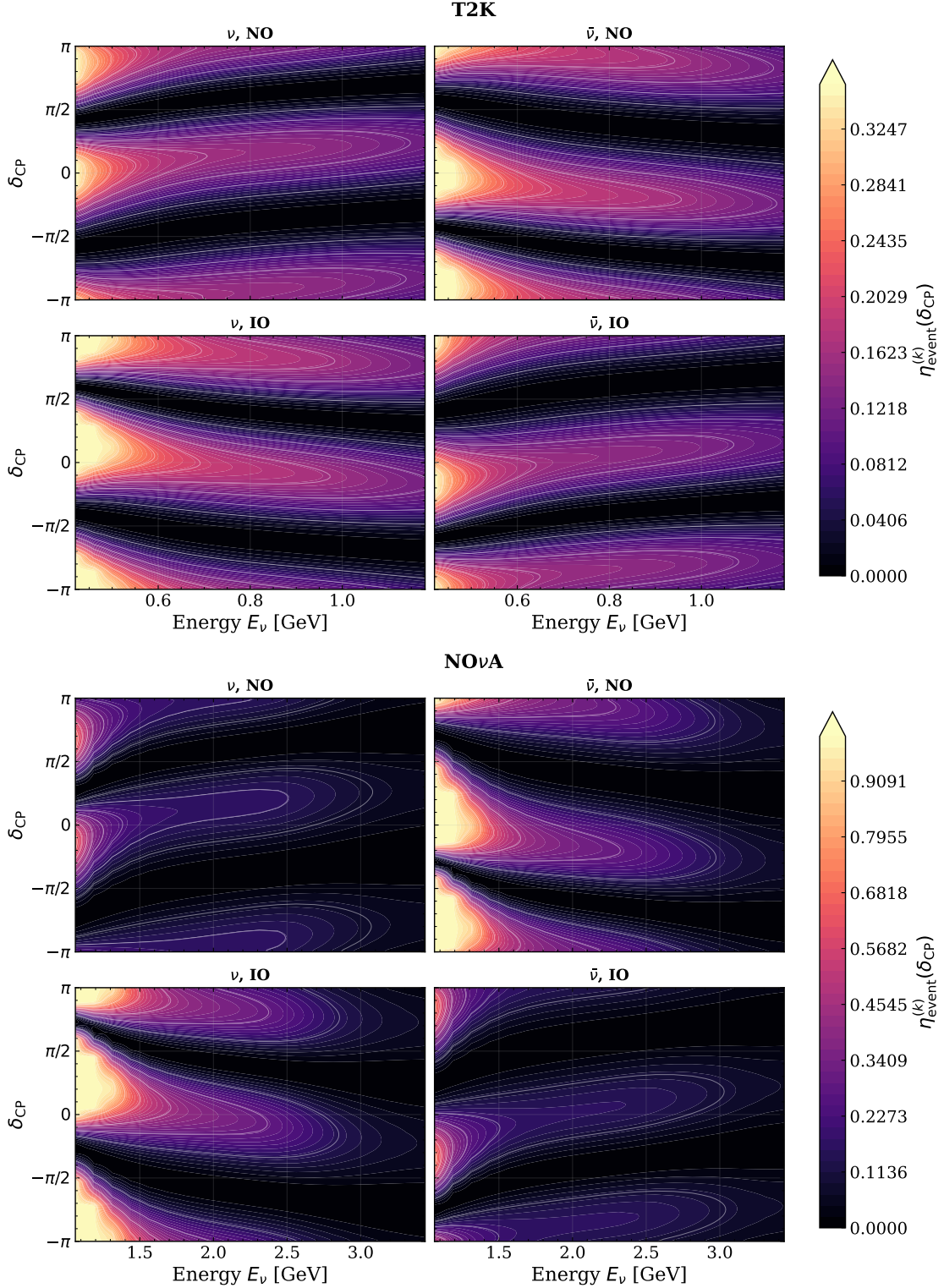


FIG. 9. Extraction efficiency  $\eta_{\text{event}}^{(k)}(\delta_{\text{CP}})$  for the T2K and NO $\nu$ A configurations. The color scale (0 to 1) indicates the fraction of the extraction efficiency that is accessible via the experimental measurement. The horizontal axis represents the neutrino energy  $E_\nu$ , and the vertical axis refers to  $\delta_{\text{CP}}$ . Panels show neutrino (left) and antineutrino (right) modes, with NO (top) and IO (bottom). See the text for a detailed explanation.

For the case of NO, the T2K configuration exhibits its maximum extraction efficiency,  $\eta_{\text{event}}^{\text{tot}} \simeq 0.18$ , around the CP-conserving values in both neutrino and antineutrino modes, while it drops sharply to  $\eta_{\text{event}}^{\text{tot}} \sim 0.02$  near  $\delta_{\text{CP}} = -\pi/2$ . Similarly, for NO $\nu$ A, the extraction efficiency reaches its maximum value,  $\eta_{\text{event}}^{\text{tot}} \simeq 0.38$ , near the CP-conserving values in the antineutrino mode, reflecting the disparity in the distribution of information across different neutrino modes. However, upon combining both beam modes, the maximal extraction efficiencies become comparable for the two experiments due to the partial cancellation of matter effects.

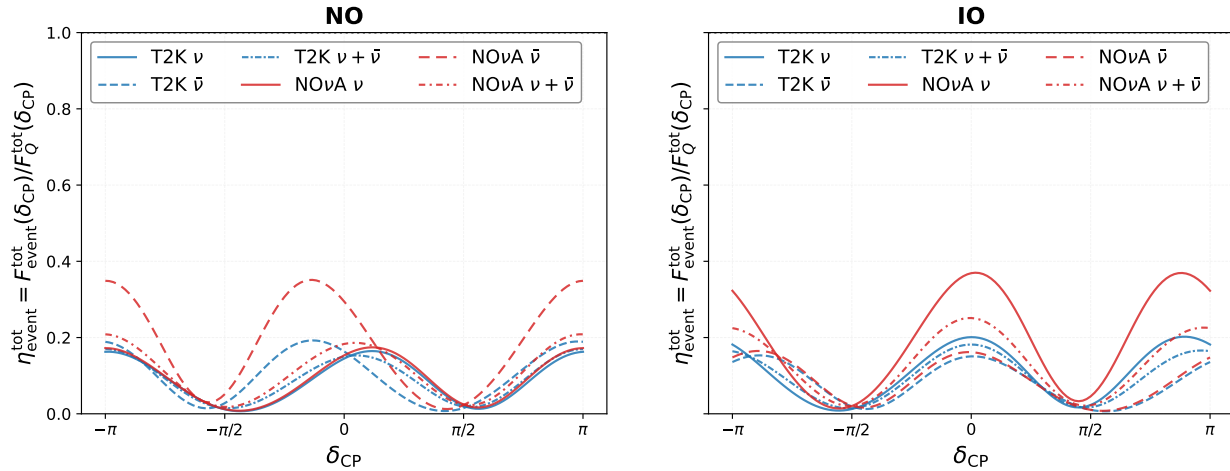


FIG. 10. Total extraction efficiency  $\eta_{\text{event}}^{\text{tot}}(\delta_{\text{CP}})$  for the T2K (blue) and NO $\nu$ A (red) configurations. For both experiments, solid lines represent the neutrino mode, dashed lines the antineutrino mode, and dot-dashed lines the combined neutrino plus antineutrino modes. See the text for a detailed explanation.

Under the assumption of IO, the T2K setup shows no significant change with the reversal of neutrino mass ordering and behaves similarly to the NO case. In contrast, for NO $\nu$ A, although the magnitude of the maximal extraction efficiency remains nearly unchanged, the dominant contribution shifts from the antineutrino mode to the neutrino mode. Upon combining both beam modes, the maximal extraction efficiency again becomes similar to that observed for NO. When combining the Fisher information for both neutrino and antineutrino mode, the overall statistical information indeed gets improved but it washes out the feature of asymmetry observed in the separate beam modes.

## VI. CONCLUSIONS AND OUTLOOK

In this work, we study the sensitivity to the leptonic CP-violating phase in the T2K and NO $\nu$ A experiments using information theory framework based on Fisher information at both the quantum and statistical event levels, with the primary goal of probing how efficiently the current generation of long-baseline experiments extracts information from measurements compared to the intrinsic quantum information encoded in the propagated neutrino states.

We first investigate the QFI associated with  $\delta_{\text{CP}}$  separately for neutrino and antineutrino states under both NO and IO. We demonstrate that, for T2K, the difference between the corresponding neutrino and antineutrino states remains comparatively small, whereas for

NO $\nu$ A the difference becomes significantly larger due to stronger matter effects. This directly indicates that the intrinsic information associated with the oscillation parameter is encoded differently in different neutrino states, and that the interaction with matter during propagation further enhances this distinction.

For the NO scenario, the neutrino state exhibits comparatively larger QFI than the corresponding antineutrino state, whereas for IO the behavior reverses and the antineutrino state shows larger QFI than the neutrino state. This indicates that the maximum amount of intrinsic quantum information relevant for the estimation of  $\delta_{\text{CP}}$  is dependent on the assumed neutrino mass ordering for a specific state. However, upon combining the neutrino and antineutrino states, the corresponding QFI becomes nearly identical and largely independent of the choice of mass ordering. We find that the QFI exhibits only a weak dependence on the value of  $\delta_{\text{CP}}$  for both neutrino and antineutrino states individually, as well as for the combined configuration, under both neutrino mass orderings.

We also define the asymmetry in QFI between the neutrino and antineutrino states, analogous to the conventional probability asymmetry,  $A_{\text{CP}}$ , for the appearance channels of  $\nu_e$  and  $\bar{\nu}_e$ . We show that the QFI asymmetry exhibits a qualitatively similar behavior to  $A_{\text{CP}}$ . For T2K, the corresponding  $A_{\text{QFI}}$  changes sign and exhibits dependence on the neutrino mass ordering, unlike the probability asymmetry. In contrast, for NO $\nu$ A both asymmetries exhibit similar behavior. This further reinforces our observation that the neutrino mass ordering affects not only the oscillation probabilities, but also the intrinsic sensitivity of the propagated quantum states to variations in  $\delta_{\text{CP}}$ .

Next, we include the corresponding event-level spectral information to construct the event-weighted QFI as an experimentally relevant benchmark for the accessible quantum information. We show that the event-weighted QFI develops localized structures around the first oscillation maximum and near the regions  $\delta_{\text{CP}} = \pm\pi/2$ , thereby exhibiting a stronger dependence on  $\delta_{\text{CP}}$  due to the reconstructed spectral shape in both T2K and NO $\nu$ A. The corresponding distributions also exhibit strong beam-mode and hierarchy dependence. For NO $\nu$ A, these features become more pronounced due to the sharper spectral peaks around the oscillation maximum and the stronger matter effects during propagation.

Using the standard statistical definition of Fisher information derived from the Poisson likelihood associated with reconstructed event measurements, we obtain the corresponding event-level Fisher information for both the T2K and NO $\nu$ A configurations. This event-level Fisher information exhibits strong dependence on neutrino energy, beam polarity, and neutrino mass ordering. We also observe that, for T2K, the information is distributed more broadly across the reconstructed energy bins compared to the corresponding event-weighted QFI distributions. In contrast, this feature is comparatively less pronounced in NO $\nu$ A due to its sharper spectral shape around the oscillation maximum. Furthermore, the experimentally accessible Fisher information becomes significantly suppressed near the maximally CP-violating values of  $\delta_{\text{CP}}$  ( $\delta_{\text{CP}} \simeq \pm\pi/2$ ). This indicates that the reconstructed event spectra in both T2K and NO $\nu$ A become comparatively less sensitive to small variations of the CP phase in these regions.

To estimate how much information is extracted in the experiments from the intrinsic quantum information present in the propagated neutrino states, we define the quantity namely, bin-wise extraction efficiency, as the ratio between the event-level Fisher information and the corresponding effective quantum benchmark given by the event-weighted QFI. The corresponding distributions follow a behavior qualitatively similar to that of the event-level Fisher information itself. The T2K configuration shows nearly identical behavior for both

neutrino mass orderings and beam polarities, whereas  $\text{NO}\nu\text{A}$  exhibits a stronger dependence on both the mass ordering and the beam mode. It should also be noted that this quantity nearly saturates the effective quantum benchmark in the very low-energy bins for all four T2K scenarios, while in  $\text{NO}\nu\text{A}$  such saturation is observed only for the antineutrino mode in NO and the neutrino mode in IO. We therefore infer that, over most of the  $(E_\nu, \delta_{\text{CP}})$  parameter space, both experiments are unable to extract the majority of the intrinsic quantum information present in the propagated neutrino states. Around the maximally CP-violating region  $\delta_{\text{CP}} \simeq -\pi/2$ , the corresponding extraction efficiency becomes negligibly small over almost the entire energy range.

We next quantify the total extraction fraction by taking the ratio of the total event-level Fisher information to the corresponding total event-weighted QFI. This quantity serves as an effective detector-level figure of merit for measuring how efficiently the complete reconstructed event spectrum extracts the available quantum information relevant for the estimation of  $\delta_{\text{CP}}$ . We find that neither T2K nor  $\text{NO}\nu\text{A}$  fully saturates the corresponding event-weighted quantum benchmark, and both experiments extract only a fraction of the intrinsic quantum information.

For the NO scenario, the maximal total extraction efficiency in the antineutrino mode remains comparatively smaller for T2K than for  $\text{NO}\nu\text{A}$  due to the stronger matter effects in the latter. Under IO, the dominant mode for information extraction shifts from the antineutrino channel to the neutrino channel, reflecting the impact of the neutrino mass ordering on the experimentally accessible information. We also show that combining the two beam modes largely removes the distinction between the mass orderings and leads to nearly identical total extraction efficiencies for both T2K and  $\text{NO}\nu\text{A}$ .

The present analysis provides a complementary framework for understanding the estimation of the leptonic CP-violating phase in neutrino oscillation experiments. We demonstrate that the sensitivity to  $\delta_{\text{CP}}$  can be understood not only through conventional statistical approaches, but also through how efficiently the detector extracts information about the parameter from the quantum state. A more robust understanding can be achieved by extending the present analysis to include all oscillation parameters together with their mutual correlations. The framework developed in this work therefore opens a new direction for comparing and optimizing future neutrino oscillation experiments based on their efficiency of quantum information extraction.

## ACKNOWLEDGMENTS

NRSC and LAD were supported in part by the Kaiping Neutrino Research Center, China. YFL was supported in part by the National Natural Science Foundation of China under Grant No. 12075255.

- 
- [1] S. Navas *et al.* [Particle Data Group], “*Review of particle physics,*” Phys. Rev. D **110** (2024) no.3, 030001
  - [2] A. Abusleme *et al.* [JUNO], “*First measurement of reactor neutrino oscillations at JUNO,*” [arXiv:2511.14593 [hep-ex]].

- [3] B. Pontecorvo, “*Inverse Beta Processes and Nonconservation of Lepton Charge*,” *Sov. Phys. JETP* **7** (1958), 172-173
- [4] Z. Maki, M. Nakagawa and S. Sakata, “*Remarks on the unified model of elementary particles*,” *Prog. Theor. Phys.* **28** (1962), 870-880
- [5] M. Schwartz, “*Feasibility of using high-energy neutrinos to study the weak interactions*,” *Phys. Rev. Lett.* **4** (1960), 306-307
- [6] T. D. Lee and C. N. Yang, “*THEORETICAL DISCUSSIONS ON POSSIBLE HIGH-ENERGY NEUTRINO EXPERIMENTS*,” *Phys. Rev. Lett.* **4** (1960), 307-311
- [7] K. Abe *et al.* [T2K], “*Constraint on the matter–antimatter symmetry-violating phase in neutrino oscillations*,” *Nature* **580** (2020) no.7803, 339-344 [erratum: *Nature* **583** (2020) no.7814, E16] [arXiv:1910.03887 [hep-ex]].
- [8] M. A. Acero *et al.* [NOvA], “*Improved measurement of neutrino oscillation parameters by the NOvA experiment*,” *Phys. Rev. D* **106** (2022) no.3, 032004 [arXiv:2108.08219 [hep-ex]].
- [9] K. Abe *et al.* [T2K], “*Measurements of neutrino oscillation parameters from the T2K experiment using  $3.6 \times 10^{21}$  protons on target*,” *Eur. Phys. J. C* **83** (2023) no.9, 782 [arXiv:2303.03222 [hep-ex]].
- [10] M. A. Acero *et al.* [NOvA], “*Expanding neutrino oscillation parameter measurements in NOvA using a Bayesian approach*,” *Phys. Rev. D* **110** (2024) no.1, 1 [arXiv:2311.07835 [hep-ex]].
- [11] S. Abubakar *et al.* [T2K and NOvA], “*Joint neutrino oscillation analysis from the T2K and NOvA experiments*,” *Nature* **646** (2025) no.8086, 818-824 [arXiv:2510.19888 [hep-ex]].
- [12] P. B. Denton, J. Gehrlein and R. Pestes, “*CP -Violating Neutrino Nonstandard Interactions in Long-Baseline-Accelerator Data*,” *Phys. Rev. Lett.* **126** (2021) no.5, 051801 [arXiv:2008.01110 [hep-ph]].
- [13] S. S. Chatterjee and A. Palazzo, “*Nonstandard Neutrino Interactions as a Solution to the NOvA and T2K Discrepancy*,” *Phys. Rev. Lett.* **126** (2021) no.5, 051802 [arXiv:2008.04161 [hep-ph]].
- [14] E. T. Jaynes, “*Information Theory and Statistical Mechanics*,” *Phys. Rev.* **106** (1957), 620-630
- [15] C. R. Rao, “*Information and the accuracy attainable in the estimation of statistical parameters*,” *Bull. Calcutta Math. Soc.* **37** (1945), 81-89.
- [16] R. A. Fisher, “*Theory of statistical estimation*,” *Math. Proc. Cambridge Philos. Soc.* **22** (1925) no.5, 700-725.
- [17] C. W. Helstrom, “*Quantum detection and estimation theory*,” *J. Stat. Phys.* **1** (1969), 231-252.
- [18] M. G. A. Paris, “*Quantum Estimation for Quantum Technology*,” *Int. J. Quant. Inf.* **7** (2009), 125-137 [arXiv:0804.2981 [quant-ph]].
- [19] J. Liu, H. Yuan, X. M. Lu and X. Wang, “*Quantum Fisher information matrix and multiparameter estimation*,” *J. Phys. A* **53** (2020) no.2, 023001 [arXiv:1907.08037 [quant-ph]].
- [20] X. M. Lu, X. Wang and C. P. Sun, “*Quantum Fisher information flow and non-Markovian processes of open systems*,” *Phys. Rev. A* **82** (2010), 042103 [arXiv:0912.0587 [quant-ph]].
- [21] L. Pezze and A. Smerzi, “*Quantum theory of phase estimation*,” [arXiv:1411.5164 [quant-ph]].
- [22] E. C. Nogueira, G. de Souza, A. D. Varizi and M. D. Sampaio, “*Quantum estimation in neutrino oscillations*,” *Int. J. Quant. Inf.* **15** (2017) no.6, 1750045 [arXiv:1610.05388 [quant-ph]].
- [23] M. Ignotti, C. Frugiuele, M. G. A. Paris and M. G. Genoni, “*Is the large uncertainty of  $\delta_{CP}$  fundamentally encoded in the neutrino quantum state?*,” [arXiv:2511.20148 [hep-ph]].

- [24] C. Frugiuele, M. G. Genoni, M. Ignati and M. G. A. Paris, “Quantum Estimation Theory Limits in Neutrino Oscillation Experiments,” [arXiv:2602.16534 [hep-ph]].
- [25] N. R. S. Chundawat and Y. F. Li, “*Information-Theoretic Gaps in Solar and Reactor Neutrino Oscillation Measurements,*” [arXiv:2602.07991 [hep-ph]].
- [26] B. Yadav, A. Subba and Y. Shi, “*Quantum Fisher Information Revealing Parameter Sensitivity in Long-Baseline Neutrino Experiments,*” [arXiv:2602.05221 [hep-ph]].
- [27] B. W. Farooq, B. Singh Koranga and A. Chatterjee, “*Quantum Fisher Information as a Probe of Sterile Neutrino New Physics: Geometric Advantage of KM3NeT over IceCube,*” [arXiv:2604.01256 [hep-ph]].
- [28] M. Blasone, F. Dell’Anno, S. De Siena, M. Di Mauro and F. Illuminati, “*Multipartite entangled states in particle mixing,*” Phys. Rev. D **77** (2008), 096002 [arXiv:0711.2268 [quant-ph]].
- [29] M. Blasone, F. Dell’Anno, S. De Siena and F. Illuminati, “*Entanglement in neutrino oscillations,*” EPL **85** (2009) no.5, 50002 [arXiv:0707.4476 [hep-ph]].
- [30] A. K. Alok, S. Banerjee and S. U. Sankar, “*Quantum correlations in terms of neutrino oscillation probabilities,*” Nucl. Phys. B **909** (2016), 65-72 [arXiv:1411.5536 [hep-ph]].
- [31] S. Banerjee, A. K. Alok, R. Srikanth and B. C. Hiesmayr, “*A quantum information theoretic analysis of three flavor neutrino oscillations,*” Eur. Phys. J. C **75** (2015) no.10, 487 [arXiv:1508.03480 [hep-ph]].
- [32] J. A. Formaggio, D. I. Kaiser, M. M. Murskyj and T. E. Weiss, “*Violation of the Leggett-Garg inequality in neutrino oscillations,*” Phys. Rev. Lett. **117** (2016) no.5, 050402 [arXiv:1602.00041 [quant-ph]].
- [33] Q. Fu and X. Chen, “*Testing violation of the Leggett-Garg-type inequality in neutrino oscillations of the Daya Bay experiment,*” Eur. Phys. J. C **77** (2017) no.11, 775 [arXiv:1705.08601 [hep-ph]].
- [34] J. Naikoo, A. K. Alok, S. Banerjee, S. U. Sankar, G. Guarnieri, C. Schultze and B. C. Hiesmayr, “*A quantum information theoretic quantity sensitive to the neutrino mass-hierarchy,*” Nucl. Phys. B **951** (2020), 114872 [arXiv:1710.05562 [hep-ph]].
- [35] J. Naikoo, A. K. Alok and S. Banerjee, “*Study of temporal quantum correlations in decohering B and K meson systems,*” Phys. Rev. D **97** (2018) no.5, 053008 [arXiv:1802.04265 [hep-ph]].
- [36] J. Naikoo, A. K. Alok, S. Banerjee and S. U. Sankar, “*Leggett-Garg inequality in the context of three flavour neutrino oscillation,*” Phys. Rev. D **99** (2019) no.9, 095001 [arXiv:1901.10859 [hep-ph]].
- [37] F. Ming, X. K. Song, J. Ling, L. Ye and D. Wang, “*Quantification of quantumness in neutrino oscillations,*” Eur. Phys. J. C **80** (2020) no.3, 275.
- [38] M. Blasone, F. Illuminati, L. Petruzzello and L. Smaldone, “*Leggett-Garg inequalities in the quantum field theory of neutrino oscillations,*” Phys. Rev. A **108** (2023) no.3, 032210 [arXiv:2111.09979 [quant-ph]].
- [39] A. K. Jha, M. Dutta, M. Pathak, S. Banerjee and B. Mukhopadhyay, “*Probing the quantum speed limit and entanglement in flavor oscillations of neutrino-antineutrino system in curved spacetime,*” Phys. Rev. D **112** (2025) no.4, 043045 [arXiv:2504.20236 [gr-qc]].
- [40] D. S. Chattopadhyay and A. Dighe, “*Quantum mismatch: A powerful measure of quantumness in neutrino oscillations,*” Phys. Rev. D **108** (2023) no.11, 112013 [arXiv:2304.02475 [hep-ph]].
- [41] M. Alam, V. Brdar and D. S. Chattopadhyay, “*Exploring Quantumness at Long-Baseline Neutrino Experiments,*” [arXiv:2601.15375 [hep-ph]].
- [42] A. K. Alok, T. J. Chall, N. R. S. Chundawat, S. Gangal and G. Lambiase, “*Quantum coherence in neutrino spin-flavor oscillations,*” Phys. Rev. D **111** (2025) no.3, 036015 [arXiv:2407.16742]

- [hep-ph]].
- [43] S. Bouri, A. K. Jha and S. Banerjee, “*Probing CP violation and mass ordering in neutrino oscillations in matter through quantum speed limits,*” Phys. Rev. D **112** (2025) no.3, 036007 [arXiv:2405.13114 [hep-ph]].
  - [44] A. K. Alok, M. Blasone, T. J. Chall, N. R. S. Chundawat and G. Lambiase, “*Coherent dynamics of flavor mode entangled neutrinos,*” [arXiv:2501.06311 [hep-ph]].
  - [45] A. K. Alok, T. J. Chall, N. R. S. Chundawat and Y. F. Li, “*Quantifying Imaginarity in Neutrino Systems,*” [arXiv:2412.01871 [hep-ph]].
  - [46] R. Banerjee, P. K. Panigrahi, H. Mishra and S. Patra, “*Concurrence fill and mode distribution of entanglement in neutrino oscillation,*” Phys. Rev. D **113** (2026) no.7, 073005 [arXiv:2512.11320 [hep-ph]].
  - [47] M. A. Nielsen and I. L. Chuang, “*Quantum Computation and Quantum Information: 10th Anniversary Edition,*” (Cambridge University Press, 2010).
  - [48] P. A. N. Machado, H. Nunokawa and R. Zukanovich Funchal, “*Testing for Large Extra Dimensions with Neutrino Oscillations,*” Phys. Rev. D **84** (2011), 013003 [arXiv:1101.0003 [hep-ph]].
  - [49] K. Abe *et al.* [T2K], “*Search for heavy neutrinos with the T2K near detector ND280,*” Phys. Rev. D **100** (2019) no.5, 052006 [arXiv:1902.07598 [hep-ex]].
  - [50] P. Chen, G. J. Ding, F. Gonzalez-Canales and J. W. F. Valle, “*Generalized  $\mu - \tau$  reflection symmetry and leptonic CP violation,*” Phys. Lett. B **753** (2016), 644-652 [arXiv:1512.01551 [hep-ph]].
  - [51] S. K. Agarwalla, S. S. Chatterjee, A. Dasgupta and A. Palazzo, “*Discovery Potential of T2K and NO $\nu$ A in the Presence of a Light Sterile Neutrino,*” JHEP **02** (2016), 111 [arXiv:1601.05995 [hep-ph]].
  - [52] D. V. Forero and P. Huber, “*Hints for leptonic CP violation or New Physics?,*” Phys. Rev. Lett. **117** (2016) no.3, 031801 [arXiv:1601.03736 [hep-ph]].
  - [53] O. G. Miranda, M. Tortola and J. W. F. Valle, “*New ambiguity in probing CP violation in neutrino oscillations,*” Phys. Rev. Lett. **117** (2016) no.6, 061804 [arXiv:1604.05690 [hep-ph]].
  - [54] P. Pasquini, S. C. Chuliá and J. W. F. Valle, “*Neutrino oscillations from warped flavor symmetry: predictions for long baseline experiments T2K, NO $\nu$ A and DUNE,*” Phys. Rev. D **95** (2017) no.9, 095030 [arXiv:1610.05962 [hep-ph]].
  - [55] M. Ghosh, S. Gupta, Z. M. Matthews, P. Sharma and A. G. Williams, “*Study of parameter degeneracy and hierarchy sensitivity of NO $\nu$ A in presence of sterile neutrino,*” Phys. Rev. D **96** (2017) no.7, 075018 [arXiv:1704.04771 [hep-ph]].
  - [56] J. Rout, M. Masud and P. Mehta, “*Can we probe intrinsic CP and T violations and nonunitarity at long baseline accelerator experiments?,*” Phys. Rev. D **95** (2017) no.7, 075035 [arXiv:1702.02163 [hep-ph]].
  - [57] V. Brdar, J. Kopp, J. Liu, P. Prass and X. P. Wang, “*Fuzzy dark matter and nonstandard neutrino interactions,*” Phys. Rev. D **97** (2018) no.4, 043001 [arXiv:1705.09455 [hep-ph]].
  - [58] F. Capozzi, S. S. Chatterjee and A. Palazzo, “*Neutrino Mass Ordering Obscured by Nonstandard Interactions,*” Phys. Rev. Lett. **124** (2020) no.11, 111801 [arXiv:1908.06992 [hep-ph]].
  - [59] A. de Gouvêa, G. Jusino Sánchez and K. J. Kelly, “*Very light sterile neutrinos at NO $\nu$ A and T2K,*” Phys. Rev. D **106** (2022) no.5, 055025 [arXiv:2204.09130 [hep-ph]].
  - [60] T. V. Ngoc, S. Cao, N. T. H. Van and P. T. Quyen, “*Stringent constraint on CPT violation with the synergy of T2K-II, NO $\nu$ A extension, and JUNO,*” Phys. Rev. D **107** (2023) no.1, 016013 [arXiv:2210.13044 [hep-ph]].

- [61] A. K. Alok, N. R. Singh Chundawat, A. Mandal and B. Soni, “Majorana CP-violating phases and NSI effects in neutrino decay,” *J. Phys. G* **51** (2024) no.8, 085006 [arXiv:2208.14881 [hep-ph]].
- [62] A. Cherchiglia, P. Pasquini, O. L. G. Peres, F. F. Rodrigues, R. R. Rossi and E. S. Souza, “Alleviating the present tension between T2K and NOvA with nonstandard neutrino interactions,” *Phys. Rev. D* **112** (2025) no.9, 093004 [arXiv:2310.18401 [hep-ph]].
- [63] X. Q. Li, H. X. Lin, J. Tang and S. Vihonen, “Ultralight dark matter in long-baseline accelerator neutrino oscillations,” [arXiv:2312.11704 [hep-ph]].
- [64] L. Konwar, J. Vardani and B. Yadav, “Violation of LGTI inequalities in the light of NOvA and T2K anomaly,” *Eur. Phys. J. C* **84** (2024) no.10, 1103 [arXiv:2401.02886 [hep-ph]].
- [65] M. A. Acero *et al.* [NOvA], “Search for CP-Violating Neutrino Nonstandard Interactions with the NOvA Experiment,” *Phys. Rev. Lett.* **133** (2024) no.20, 201802 [arXiv:2403.07266 [hep-ex]].
- [66] X. Y. Yu, Z. Guan, U. Rahaman and N. Ilic, “Update on non-unitary mixing in the recent NOvA and T2K data,” *Nucl. Phys. B* **1023** (2026), 117303 [arXiv:2501.00146 [hep-ph]].
- [67] C. A. Ternes and G. Pagliaroli, “Invisible neutrino decay at long-baseline neutrino oscillation experiments,” *Phys. Rev. D* **109** (2024) no.7, L071701 [arXiv:2401.14316 [hep-ph]].
- [68] G. Alonso-Álvarez, J. M. Cline, B. Laurent and U. Rahaman, “Dark photon distortions of NOvA and T2K neutrino oscillations,” *Eur. Phys. J. C* **85** (2025) no.6, 635 [arXiv:2407.13817 [hep-ph]].
- [69] G. F. S. Alves, H. Nunokawa and R. Zukanovich Funchal, “Impact of New Physics on the JUNO-Long-Baseline Synergy in Neutrino Mass Ordering Determination,” [arXiv:2603.17181 [hep-ph]].
- [70] P. B. Denton and S. J. Parke, “Smallness of matter effects in long-baseline muon neutrino disappearance,” *Phys. Rev. D* **109** (2024) no.5, 053002 [arXiv:2401.10326 [hep-ph]].
- [71] P. Huber, M. Lindner and W. Winter, “From parameter space constraints to the precision determination of the leptonic Dirac CP phase,” *JHEP* **05** (2005), 020 [arXiv:hep-ph/0412199 [hep-ph]].
- [72] H. Nunokawa, S. J. Parke and R. Zukanovich Funchal, “Another possible way to determine the neutrino mass hierarchy,” *Phys. Rev. D* **72** (2005), 013009 [arXiv:hep-ph/0503283 [hep-ph]].
- [73] Y. F. Li, J. Cao, Y. Wang and L. Zhan, “Unambiguous Determination of the Neutrino Mass Hierarchy Using Reactor Neutrinos,” *Phys. Rev. D* **88** (2013), 013008 [arXiv:1303.6733 [hep-ex]].
- [74] F. An *et al.* [JUNO], “Neutrino Physics with JUNO,” *J. Phys. G* **43** (2016) no.3, 030401 [arXiv:1507.05613 [physics.ins-det]].
- [75] B. Abi *et al.* [DUNE], “Deep Underground Neutrino Experiment (DUNE), Far Detector Technical Design Report, Volume II: DUNE Physics,” doi:10.2172/1599307 [arXiv:2002.03005 [hep-ex]].
- [76] K. Abe *et al.* [Hyper-Kamiokande], [arXiv:1805.04163 [physics.ins-det]].
- [77] A. Alekou, E. Baussan, A. K. Bhattacharyya, N. Blaskovic Kraljevic, M. Blennow, M. Bogomilov, B. Bolling, E. Bouquerel, O. Buchan and A. Burgman, *et al.* *Eur. Phys. J. ST* **231** (2022) no.21, 3779-3955 [erratum: *Eur. Phys. J. ST* **232** (2023), 15-16] [arXiv:2206.01208 [hep-ex]].
- [78] M. Blennow, P. Coloma, A. Donini and E. Fernandez-Martinez, “Gain fractions of future neutrino oscillation facilities over T2K and NOvA,” *JHEP* **07** (2013), 159 [arXiv:1303.0003 [hep-ph]].

- [79] A. Cabrera, Y. Han, M. Obolensky, F. Cavalier, J. Coelho, D. Navas-Nicolás, H. Nunokawa, L. Simard, J. Bian and N. Nayak, *et al.* “*Synergies and prospects for early resolution of the neutrino mass ordering,*” *Sci. Rep.* **12** (2022) no.1, 5393 [arXiv:2008.11280 [hep-ph]].
- [80] L. A. Delgadillo and O. G. Miranda, “*Future leptonic CP phase determination in the presence of NSI,*” *Phys. Rev. D* **108** (2023) no.9, 095024 [arXiv:2304.05545 [hep-ph]].
- [81] S. J. Parke and R. Zukanovich-Funchal, “*Mass ordering sum rule for the neutrino disappearance channels in T2K, NOvA, and JUNO,*” *Phys. Rev. D* **111** (2025) no.1, 013008 [arXiv:2404.08733 [hep-ph]].
- [82] S. Goswami, A. Gupta, U. Rahaman and S. K. Raut, “*Enhancing the sensitivity to neutrino oscillation parameters using synergy between T2K, NOvA and JUNO,*” [arXiv:2512.00172 [hep-ph]].
- [83] G. Cowan, “*Statistical data analysis*”.
- [84] P. Huber, M. Lindner and W. Winter, “*Simulation of long-baseline neutrino oscillation experiments with GLoBES (General Long Baseline Experiment Simulator),*” *Comput. Phys. Commun.* **167** (2005), 195 [arXiv:hep-ph/0407333 [hep-ph]].
- [85] P. Huber, J. Kopp, M. Lindner, M. Rolinec and W. Winter, “*New features in the simulation of neutrino oscillation experiments with GLoBES 3.0: General Long Baseline Experiment Simulator,*” *Comput. Phys. Commun.* **177** (2007), 432-438 [arXiv:hep-ph/0701187 [hep-ph]].
- [86] P. Huber, M. Lindner and W. Winter, “*Superbeams versus neutrino factories,*” *Nucl. Phys. B* **645** (2002), 3-48 [arXiv:hep-ph/0204352 [hep-ph]].
- [87] I. Esteban, M. C. Gonzalez-Garcia, M. Maltoni, I. Martinez-Soler, J. P. Pinheiro and T. Schwetz, “*NuFit-6.0: updated global analysis of three-flavor neutrino oscillations,*” *JHEP* **12** (2024), 216 [arXiv:2410.05380 [hep-ph]].